

**Enhancement of Non Linear Optical
(NLO) responses of Germanium Doped
Graphdiyne modulated by Superalkali
clusters**



By

Shaista Jabeen

NUST00000328714

Supervisor

Dr.Fouzia Perveen Malik

School of Interdisciplinary Engineering & Science (SINES)

National University of Sciences and Technology (NUST)

Islamabad, Pakistan

September 2024

**Enhancement of Non Linear Optical
(NLO) responses of Germanium Doped
Graphdiyne modulated by Superalkali
clusters**



By

Shaista Jabeen

NUST00000328714

Supervisor

Dr.Fouzia Perveen Malik

A thesis submitted in partial fulfillment of the

requirements for the degree of

Master of Science in

Computational Science and Engineering

School of Interdisciplinary Engineering & Science (SINES)

National University of Sciences and Technology (NUST)

Islamabad, Pakistan

September 2024

Approval

It is certified that the contents and form of the thesis entitled “**Enhancement of Non Linear Optical (NLO) responses of Germanium Doped Graphdiyne modulated by superalkali clusters**” submitted by **Shaista Jabeen** have been found satisfactory for the requirement of the degree.

Advisor: **Dr. Fouzia Parveen Malik**

Signature: _____

Date: _____

Committee Member 1: **Dr. Mian Ilyas**

Signature: _____

Date: _____

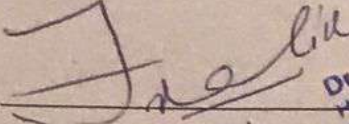
Committee Member 2: **Dr. Faheem Amin**

Signature: _____

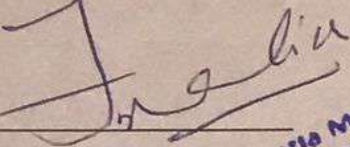
Date: _____

THESIS ACCEPTANCE CERTIFICATE

Certified that final copy of MS/MPhil thesis written by Mr/Ms SHAISTA JABEEN Registration No. 00000328714 of SINES has been vetted by undersigned, found complete in all aspects as per NUST Statutes/Regulations, is free of plagiarism, errors, and mistakes and is accepted as partial fulfillment for award of MS/MPhil degree. It is further certified that necessary amendments as pointed out by GEC members of the scholar have also been incorporated in the said thesis.

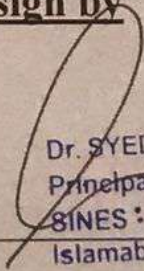
Signature with stamp: 
Name of Supervisor: Dr. Fouzia Malik
Date: 25-9-2024

Dr Fouzia Malik
HoD Sciences
Professor
SINES, NUST
Islamabad

Signature of HoD with stamp: 
Date: 25-9-2024

Dr Fouzia Malik
HoD Sciences
Professor
SINES, NUST
Islamabad

Countersign by

Signature (Dean/Principal): 
Date: 25/9/24

Dr. SYED IRTIZA ALI SHAH
Principal & Dean
SINES : NUST, Sector H-12
Islamabad

Dedication

I dedicate this research to my parents, whose unwavering support, boundless encouragement, and sacrifices have been the foundation of my academic journey. To my husband, whose love, patience, and understanding have provided me with the strength and motivation to persevere through every challenge. Your belief in me has been a constant source of inspiration and has made this achievement possible. Thank you for being my rock and guiding light. Also it is dedicated to all of my friends especially Minahil , Rimsha who have supported, inspired, and challenged me throughout this journey. Your unwavering encouragement, insightful feedback, and camaraderie have been invaluable and lastly my mentor Atif Rehman whose collaboration, expertise, and dedication have enriched my experience and made this achievement possible. I am grateful for the shared knowledge and the spirit of teamwork.

Certificate of Originality

I hereby declare that this submission is my own work and to the best of my knowledge it contains no materials previously published or written by another person, nor material which to a substantial extent has been accepted for the award of any degree or diploma at adviserAffiliation at school or at any other educational institute, except where due acknowledgement has been made in the thesis. Any contribution made to the research by others, with whom I have worked at school or elsewhere, is explicitly acknowledged in the thesis. I also declare that the intellectual content of this thesis is the product of my own work, except for the assistance from others in the project's design and conception or in style, presentation and linguistics which has been acknowledged.

Author Name: **Shaista Jabeen**

Signature: _____

Acknowledgment

I begin by expressing deep gratitude to the Almighty Allah for His abundant blessings and guidance throughout this journey. I want to take this moment to extend my sincere appreciation to all those who contributed to the completion of my master's thesis. Their unwavering support, guidance, and encouragement were instrumental in ensuring the success of my research.

First and foremost, I am immensely thankful to my supervisor, Dr. Fouzia Perveen Malik, for her outstanding leadership during this journey. Her invaluable input, insightful questioning, and constructive suggestions significantly enhanced the quality of this thesis. I would like to thank to my Guidance committee members Dr Fahim Ameen (SNS, NUST) and Dr Mian Ilyas Ahmad (SINES, NUST) whose guidance from the initial step in research enabled me to develop an understanding of the subject.

I would like to express my gratitude to Principal SINES Dr.Hammad Cheema for providing the ADF software that made it possible for me to conduct this study. I am also very appreciative of the advice and inspiration I have received from the SINES faculty members and my lab colleagues.

Shiasta Jabeen

Abstract

Functionalized graphdiyne (GDY) structures doped with Germanium atoms and adsorbed with AM_3O units ($AM = Li, Na, K$) have been studied using DFT calculations to explore their NLO properties as potential optical materials. The AM_3O units exhibit strong interactions with Ge-GDY clusters, evidenced by the large binding energies, particularly for the Li-adsorbed complex (-3.06 eV), while K_3O -adsorbed Ge-GDY is stabilized by van der Waals interactions. The HOMO-LUMO gaps were 0.506 eV, 0.437 eV, and 0.231 eV for $Li_3O@Ge-GDY$, $Na_3O@Ge-GDY$, and $K_3O@Ge-GDY$, respectively. Additionally, superalkali adsorption on Ge-doped GDY reduces the H-L gap across all complexes. Results show that AM_3O adsorption onto Ge-GDY significantly lowers the vertical ionization potential (VIP), with intramolecular charge transfer playing a key role in the nonlinear optical (NLO) properties. Notably, the doped complexes exhibit exceptional NLO responses, with first hyperpolarizability values ranging from 2.83×10^4 au to 5.39×10^6 au, compared to pure graphdiyne. In conclusion, AM_3O adsorption onto Ge-GDY optimizes the NLO response of GDY-based materials provides a foundation for future research aimed at further modifications and practical applications, leveraging these insights to develop materials with tailored optical characteristics for cutting-edge technologies.

Contents

1	Introduction	1
1.1	Overview of Nonlinear Optical (NLO) Materials	1
1.1.1	Types of NLO Materials	1
1.1.2	Importance of NLO materials in modern technology	2
1.1.3	Application of NLO materials	2
1.2	Introduction to Graphdiyne	3
1.2.1	Structure and Composition of GDY	3
1.2.2	Synthesis Methods for GDY	4
1.3	Fundamental Properties of GDY	4
1.3.1	Electronic Structure and Conductivity	4
1.3.2	Mechanical properties	5
1.3.3	Application of GDY	5
1.4	Doping of GDY	6
1.5	Superalkalis	6
1.6	Mechanisms for Enhancing NLO Responses	7
1.6.1	Electron Push–Pull Mechanism	7
1.6.2	Metal Ligand Framework	7
1.6.3	Excess Electrons Strategy	8
1.7	Computational Chemistry in NLO Studies	8
1.7.1	Computational Methods and Models	9

CONTENTS

2	Literature Review	10
2.1	State of the Art	10
2.2	Problem Statement	19
2.3	Solution statement	19
2.4	Research Goals and Aims	19
3	Methodology	20
3.1	Computational Simulation Suite	20
3.2	Classical Mechanical Method	20
3.2.1	Molecular Mechanics	20
3.2.2	Molecular Dynamics	21
3.3	Quantum Mechanical Method	21
3.3.1	Wave Functional based Theory	21
3.3.2	Density Functional Theory	21
3.3.3	The Hohenberg-Kohn theorem	22
3.3.4	Kohen- Sham Equations	22
3.4	ADF Simulation Suite	23
3.5	Computational Tool	23
3.5.1	Functionality	24
3.5.2	The Hohenberg-Kohn theorem	24
3.5.3	Exchange Coorelation Functionals	25
3.5.4	The Local Density Approximation	25
3.5.5	Generalized Gradient approximations	25
3.6	Methodology	26
4	Results And Discussion	28
4.1	Quantum Mechanical Investigation of graphdiyne	28
4.2	Geometry Optimization	28

CONTENTS

4.3	Adsorption Energy	29
4.3.1	Adsorption behavior at elevated temperature i-e 323 K	32
4.4	Frontier molecular orbital(FMO) analysis	34
4.5	Charge Transfer mechanism	36
4.5.1	Natural Bond Orbital(NBO) analysis	36
4.5.2	Natural Population Analysis	37
4.6	Nonlinear optical properties	37
4.7	Electrical Conductivity	39
4.8	Global Quantum Chemical Descriptors	41
5	Conclusion	42
	References	43

List of Tables

2.1	Polarizability (α_0) in au, first hyperpolarizability (β_0) in au, change in dipole moment ($\Delta\mu$) in Debye, oscillator strength (f_0) in au, transition energy (ΔE) in eV, and second order hyperpolarizability (β_{vec}) of superalkali-doped graphdiyne ($M_2X@GDY$) complexes.	12
4.1	The adsorption energy values of GDY clusters at 298 K	34
4.2	The adsorption energy values of superalkali clusters at 313 K	34
4.3	HOMO-LUMO energy values of pristine and Ge doped GDY clusters of superalkalis	36
4.4	Charge values for different clusters adsorbed on GDY.	37
4.5	Calculated vertical ionization potentials (VIP), the HOMO-LUMO gaps (E_g), mean dipole moment (μ_o) in a.u., static polarizability (α_o) in a.u., the static first hyperpolarizability (β) _{tot} in a.u.	39
4.6	Electronic parameters and electrical conductivity of Ge-GDYs	40
4.7	Global indices for the complexes	41

List of Figures

1.1	Applications of Nonlinear Optical Materials Across Various Fields	3
1.2	(a)Graphene (b) a-graphyne; (c) b-graphyne; (d) g-graphyne; (e) 6,6,12-graphyne; (f) b-graphdiyne; and (g) Graphdiyne	4
1.3	Donor- π -acceptor	8
1.4	Methods of computational chemistry	9
2.1	Schematic diagram of a functionalized graphdiyne (GDY) sheet adsorbed by the tetrahedral Li_3NM ($\text{M} = \text{Li}, \text{Na}, \text{K}$) alkalide complex	11
2.2	ELF and LOL analysis of $\text{Li}@2\text{N-BNNC}$, $\text{Li}@2\text{B-BNNC}$, and $\text{Li}@\text{BN-BNNC}$	13
2.3	Optimized geometries with HOMO-LUMO densities of $\text{Li}_3\text{O@[12-crown-4]M}$ complexes.	13
2.4	PDOS for Al/BP nanocages doped with various alkaline earth metals	14
2.5	Optimized structures of the most stable mixed-superalkali-doped $\text{B}_{12}\text{N}_{12}$ com- plexes, as adapted from Bano et al. (2022), with permission from the Royal Society of Chemistry	15
2.6	Optimized structures of alkali-doped AIP nano-cages ($\text{MAI}_{12}\text{P}_{11}$ and $\text{MAI}_{11}\text{P}_{12}$), with all bond lengths expressed in Angstroms.	16
3.1	Step-based methodology for current research	27
4.1	[a]Optimized geometry of pristine GDY, [b]Energy graph of pristine GDY cal- culated at TZ basis set at GGA: PBE/DFT performed at ADF modelling suite	29

LIST OF FIGURES

4.2	[a] Optimized geometry of Ge doped GDY, [b]Energy graph of Ge doped GDY calculated at TZ basis set at GGA: PBE/DFT performed at ADF modelling suite	30
4.3	[a] Optimized geometry of Li ₃ O on Ge doped GDY and [b]energy graph of Li ₃ O on Ge doped GDY calculated at TZ basis set at GGA: PBE/DFT performed at ADF modelling suite	31
4.4	[a] Optimized geometry of Na ₃ O on Ge doped GDY and [b]energy graph of Na ₃ O on Ge doped GDY calculated at TZ basis set at GGA: PBE/DFT performed at ADF modelling suite	32
4.5	[a] Optimized geometry of K ₃ O on Ge doped GDY and [b]energy graph of K ₃ O on Ge doped GDY calculated at TZ basis set at GGA: PBE/DFT performed at ADF modelling suite	33
4.6	HOMO-LUMO representation of (a)pristine GDY (b)Ge-GDY	35
4.7	HOMO-LUMO representation of(a)Li ₃ O/Ge-GDY (b)Na ₃ O/Ge-GDY (c)K ₃ O/Ge-GDY	35
4.8	Charge Analysis of(a)Li ₃ O/Ge-GDY (b)Na ₃ O/Ge-GDY (c)K ₃ O/Ge-GDY	38

List of Abbreviations and Symbols

Abbreviations

GDY	graphdiyne
DFT	Density Functional Theory
MM	Molecular Mechanics
GGA	Generalized Gradient Approximation
LDA	Local Density Approximation
SCF	Self Consistent Field

CHAPTER 1

Introduction

1.1 Overview of Nonlinear Optical (NLO) Materials

Nonlinear optics is a dynamic and versatile field of science that describe the interaction between light and matter, where the induced polarization depends nonlinearly on external electric and magnetic fields[2].Nonlinear optical (NLO) materials are substances that exhibit a nonlinear response to optical fields, meaning their optical properties change in a non-proportional manner with the intensity of the incident light. These materials can generate new frequencies, alter the phase and amplitude of light waves, and enable phenomena such as second-harmonic generation, third-harmonic generation, and the Kerr effect.In 1960, the invention of the first Ruby laser by Maiman sparked fresh interest in the field of nonlinear optics [1]. NLO materials are essential in applications like frequency conversion, optical switching, and signal processing in photonics.

1.1.1 Types of NLO Materials

Organic Materials:

Organic NLO materials, such as polymers and molecular crystals, offer high nonlinear coefficients and fast response times. They are often used in applications requiring large second-order nonlinearities, such as electro-optic modulators and frequency doublers.[4]

Inorganic Materials:

Inorganic crystals like lithium niobate (LiNbO_3), potassium titanyl phosphate (KTP), and barium borate (BBO) are widely used due to their robustness and high optical damage thresholds.

These materials are crucial for applications involving high-power lasers and frequency conversion.[3]

Nano structured materials:

Nano materials, including quantum dots, nano wires, and graphene-based structures, exhibit enhanced nonlinearities due to quantum confinement effects and large surface-to-volume ratios. These materials are promising for ultra-fast photonic applications and on-chip optical processing.[30]

Hybrid Materials:

Combining organic and inorganic components, hybrid NLO materials aim to leverage the strengths of both types.[24] These materials often exhibit improved mechanical properties, stability, and enhanced nonlinear responses.

1.1.2 Importance of NLO materials in modern technology

Nonlinear optical (NLO) materials are crucial in advancing photonics technology. Researchers aim to enhance the performance of optical devices by developing materials with superior nonlinear optical properties, including inorganic semiconductors, polymeric systems, and various organic molecules. Organic materials, in particular, are highly attractive due to their significant nonlinear optical properties and the versatility of synthesis methods, which allow for optimization of molecular structures to maximize nonlinear responses. The field of nonlinear optics has become a Frontier area in the fields of ultrafast pulse measurement [27], light generation and modulation [32], optical parametric amplification [39], laser frequency conversion [28], modulators [8], and optical switches [31]

1.1.3 Application of NLO materials

Nonlinear optics have impressive applications in various fields, including dynamic image processing, sensing, high-resolution imaging, optical computing, optical fiber communication, optical data storage, and materials analysis. In biology, nonlinear optics are used in microscopic imaging and photo dynamic therapy, making them particularly valuable for these applications. Some major applications of nonlinear optical materials are represented in Figure 1.1

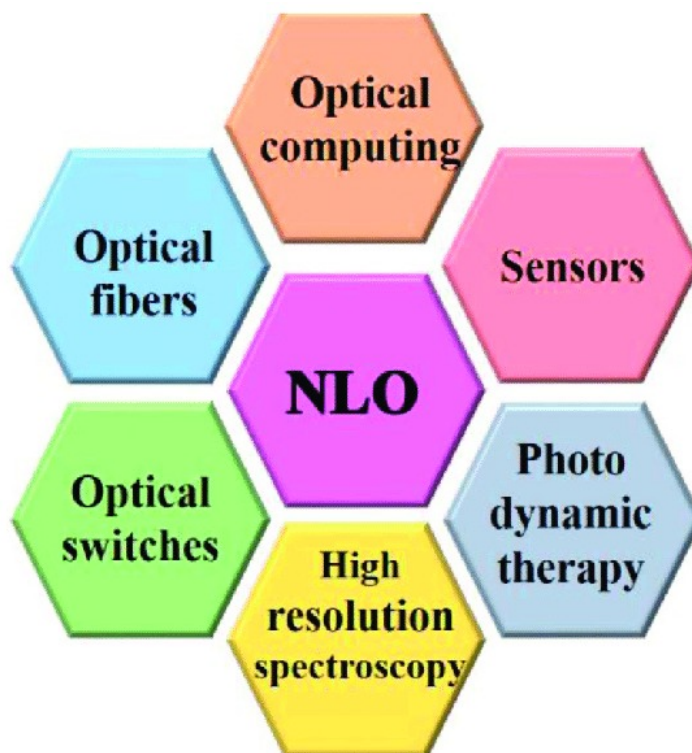


Figure 1.1: Applications of Nonlinear Optical Materials Across Various Fields

1.2 Introduction to Graphdiyne

Graphdiyne (GDY) is an intriguing and relatively novel carbon allotrope, distinguished by its unique structural composition and promising material properties. Unlike its well-known counterparts such as graphene, diamond, and carbon nanotubes, GDY features a distinctive arrangement of benzene rings interconnected by acetylenic linkers—chains of carbon atoms connected by alternating single and triple bonds.[33]

1.2.1 Structure and Composition of GDY

The fundamental building blocks of GDY are benzene rings, each consisting of six carbon atoms arranged in a hexagonal pattern. These benzene rings are linked by acetylenic chains ($-CC-$), forming a two-dimensional lattice. The variations in the number of acetylenic linkers between benzene rings give rise to different types of GDY, such as graphyne (GY), GDY, and graphtriyne (GTY).[29] These variations influence the material's electronic and mechanical properties, offering a broad spectrum of potential applications.

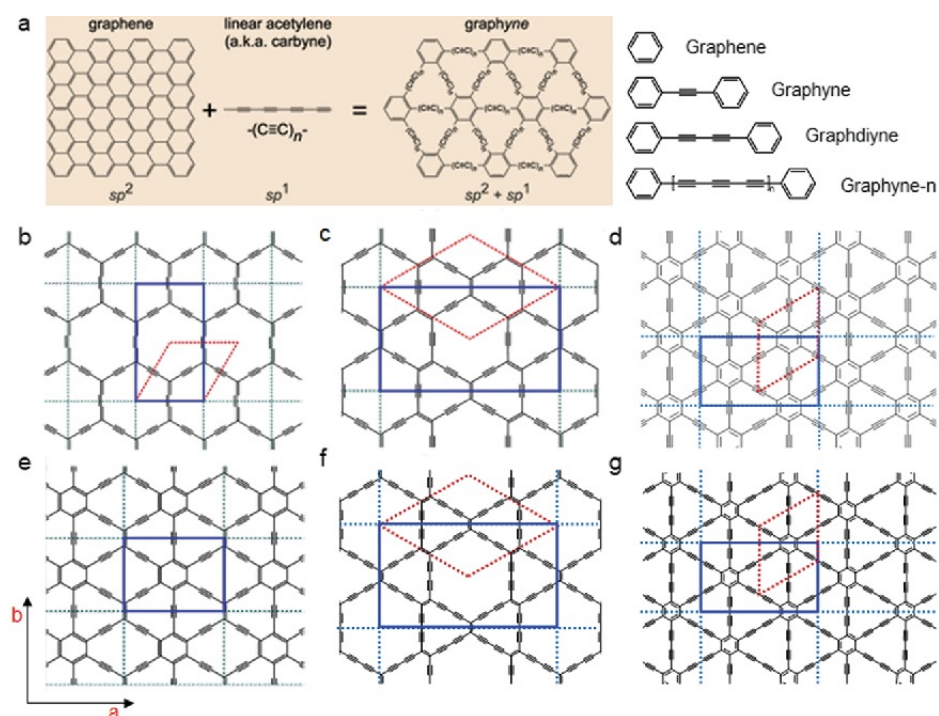


Figure 1.2: (a) Graphene (b) a-graphyne; (c) b-graphyne; (d) g-graphyne; (e) 6,6,12-graphyne; (f) b-graphdiyne; and (g) Graphdiyne

1.2.2 Synthesis Methods for GDY

The synthesis of GDY typically involves bottom-up approaches, where smaller organic molecules are assembled into the larger GDY structure. Methods such as chemical vapor deposition (CVD) and solution-based chemical reactions are commonly employed.[26] These techniques allow for precise control over the material's composition and structure, enabling the tailoring of properties for specific applications.

1.3 Fundamental Properties of GDY

1.3.1 Electronic Structure and Conductivity

GDY's unique structure imparts it with remarkable electronic properties. The sp² and sp hybridized carbon atoms result in a material that combines the high conductivity of sp² hybridized carbon (found in graphene) with the flexibility and diverse chemical reactivity of sp-hybridized carbon. This combination allows GDY to exhibit semiconductor behavior with a tunable band gap, making it a highly attractive material for electronic and optoelectronic applications.[14]

1.3.2 Mechanical properties

After the prediction of GDY's structure, its mechanical properties became a focal point of extensive study. GDY is known for its high stiffness and strength, comparable to graphene.[13] This arises from its sp and sp^2 hybridized carbon atoms arranged in a 2D lattice, which forms strong covalent bonds.

Despite its rigidity, GDY can be tailored to have certain degrees of flexibility depending on its structural modifications, such as doping or functionalization. Moreover, GDY's mechanical properties are noteworthy. The presence of both rigid benzene rings and flexible acetylenic linkers grants it a balance between strength and elasticity. This structural flexibility enables GDY to form various curved and complex shapes, which can be advantageous in nanotechnology and materials science.

1.3.3 Application of GDY

GDY exhibits an excellent π -conjugated structure, a well-distributed pore network, and adjustable electronic properties due to its sp^2 and sp hybridized flat framework. These fascinating structural and electronic characteristics suggest that GDY-based materials hold potential applications in various fields, including catalysis, rechargeable batteries, solar cells, electronic devices, magnetism, detectors, biomedicine, therapy, gas separation, and water purification. Numerous studies have already demonstrated the practical applications of GDY experimentally.

Catalysts

High-performance carbon-based catalysts typically require a large surface area, a well-defined pore structure, and stability. GDY, with its two-dimensional conjugated and highly porous plane, meets these criteria effectively. This structure increases the number of reactive sites available for specific reactions and provides an atomic-level dispersion framework for other efficient catalysts. Over the past decade, many GDY-based catalysts have been developed, showcasing significant application potential in fields such as photocatalysis, electrochemical, and photoelectrochemical water splitting reactions.

Electrocatalysts

GDY and its derivatives, featuring non-equivalent distorted rather than hexagonal symmetry Dirac cones, are theoretically predicted to exhibit superior electronic properties compared to graphene. The maximum pore size of approximately 2.5 Å facilitates the diffusion of air into

the pores of GDY when exposed to the atmosphere. Theoretical simulations suggest that the butadiyne units in GDY can induce positive charging of certain carbon atoms, enabling GDY to function as a metal-free catalyst for oxygen reduction reactions (ORR).

Nitrogen doping further enhances the electrocatalytic properties of GDY. N-doped GDY exhibits competitive electrocatalytic activity comparable to that of platinum/carbon (Pt/C) catalysts, along with superior stability and tolerance[26]. Quantum mechanical calculations reveal that nitrogen doping induces a significant positive charge on the carbon atoms adjacent to nitrogen atoms, facilitating electron withdrawal from the anode and thereby enhancing ORR activity. This improvement makes N-doped GDY a promising material for various electrocatalytic applications, including fuel cells and metal-air batteries.

1.4 Doping of GDY

Doping involves introducing impurity atoms into a material to alter its electronic, optical, and structural properties. It creates hybrid materials, combining the flexibility of organic molecules with the robustness of inorganic crystals. Due to the remarkable properties of the GDY material, the characterization and manipulation of dopants in GDY have led to a wide range of applications such as frequency doubling (second-harmonic generation, SHG) or frequency mixing. It allows for the introduction of specific functional groups or atoms to achieve desired NLO properties, making the material highly customizable. Doping can also induce or enhance asymmetry in the crystal structure and increase the dipole moment, both of which boost the nonlinear optical response.

1.5 Superalkalis

Superalkalis are a class of theoretical and synthetic compounds characterized by their exceptionally low ionization energies, even lower than those of the most electropositive alkali metals. The examples of typical superalkali cations include FLi_2^+ , OLi_3^+ , NLi_4^+ , etc.[17] This unique property allows superalkalis to act as powerful electron donors, making them highly reactive. Due to their strong electron-donating properties, superalkalis can significantly enhance the nonlinear optical properties of materials. This makes them valuable in the design of advanced NLO materials for applications in telecommunications, data storage, and laser technology. They may also be explored for use in batteries and other energy storage devices due to their

ability to donate electrons readily. Here we are using alkali metal oxides (AM_3O) where $AM=(Li, Na, K)$ on the surface of GDY as adsorbate.

1.6 Mechanisms for Enhancing NLO Responses

With the discovery and diverse applications of nonlinear optics, researchers have been working on enhancing the NLO response of various inorganic and organic materials. Several approaches have been established for tuning the NLO response of materials. These include implementing electron donor-acceptor push-pull mechanisms, designing octupolar molecules, introducing diffuse excess electrons, using multi-decker sandwich clusters, applying bond length alteration theory, and designing metal-organic frameworks (MOFs), among others [37]. Some of these strategies are listed here.

1.6.1 Electron Push-Pull Mechanism

The electron push-pull strategy, pioneered by Zyss and colleagues [5], focuses on enhancing the nonlinear optical properties of organic chromophores, such as stilbenes, porphyrins, and paracyclophanes [9] [11]. The molecular structure of these organic compounds plays a crucial role in shaping their nonlinear optical characteristics. When donor and acceptor groups are connected via π -bonds, they form a conjugated (D- π -A) system. This configuration, known as a push-pull mechanism, facilitates intermolecular charge transfer (ICT) from the donor to the acceptor through π -bonding shown in Figure 1.3. This process induces polarization in the presence of light and an electric field. A prominent example of such nonlinear optical (NLO) chromophores is DANS (4-[N,N-dimethylamino]-4-nitrostilbene), which exhibits intramolecular charge transfer (ICT).

1.6.2 Metal Ligand Framework

A metal-ligand framework for nonlinear optical (NLO) response involves coordinating metal ions with organic or inorganic ligands to create a network that enhances NLO properties. The coordination geometry plays a crucial role by influencing the electronic distribution and polarizability, which impacts the NLO response. Different metal ions can introduce various electronic properties and oxidation states, affecting the framework's overall hyperpolarizability. Additionally, the characteristics of the ligands, such as electron-donating or electron-withdrawing groups,



Figure 1.3: Donor- π -acceptor

modulate the electronic structure to enhance NLO properties. The interaction distance between the metal and the ligand affects the interaction strength, influencing the NLO response. Furthermore, the presence of conjugated systems within the ligands or between the metal and ligands enhances the delocalization of electrons, increasing the static polarizability and first hyperpolarizability values. By carefully designing and selecting metal-ligand combinations, researchers can create frameworks with optimized NLO properties for applications in photonics, optoelectronics, and related fields.

1.6.3 Excess Electrons Strategy

Introducing excess electrons into various systems is a novel approach that significantly enhances their nonlinear optical (NLO) properties. Both organic and inorganic systems can experience a boosted NLO response due to the presence of excess electrons[19].The substantial effect of excess electrons on clusters' hyperpolarizability has opened new possibilities for designing and preparing innovative nonlinear optical (NLO) molecular materials. Doping metal atoms (alkali, alkaline, and transition metals) onto complexants is an efficient approach to creating compounds with excess electrons.

1.7 Computational Chemistry in NLO Studies

Computational chemistry plays a pivotal role in the study and development of nonlinear optical (NLO) materials. It utilizes theoretical methods and computer software to model and predict the properties and behaviors of molecules, which is crucial for understanding and enhancing their NLO responses[10].Computational chemistry is an indispensable tool in the field of NLO stud-

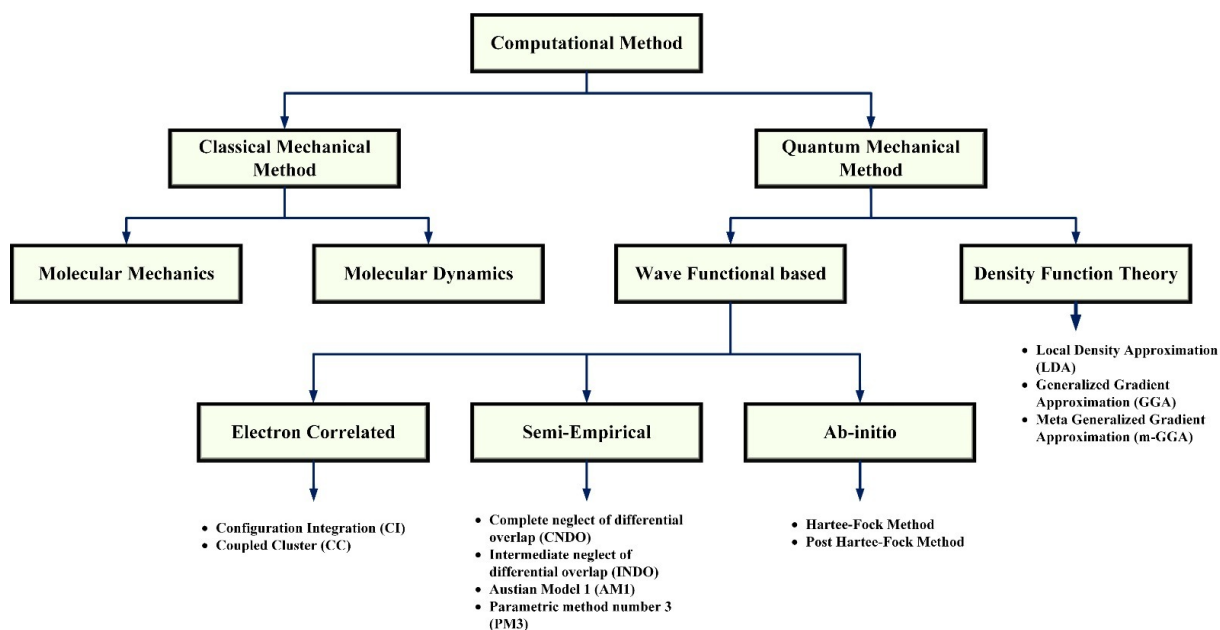


Figure 1.4: Methods of computational chemistry

ies. By leveraging various theoretical approaches, it enables the accurate prediction and rational design of novel materials with superior nonlinear optical properties, thereby driving advancements in photonics, telecommunications, and other related technologies.

1.7.1 Computational Methods and Models

Computational chemistry employs theoretical methods using computer software to determine the structures and characteristics of molecules. Major approaches in quantum chemistry include molecular mechanics, ab-initio, semi-empirical, and electronic structure methods. Figure 1.4 illustrates these computational chemistry methods."

Literature Review

2.1 State of the Art

Advancements in nonlinear optical (NLO) materials have been substantial over the past few decades, driven by the need for improved performance in telecommunications, data storage, and photonic devices. Researchers have developed a variety of organic and inorganic NLO materials with enhanced properties. Organic materials, such as conjugated polymers and small molecules, have seen significant improvements in their NLO coefficients due to advanced molecular engineering techniques. Inorganic materials, including crystals like lithium niobate and new two-dimensional materials such as graphene and its derivatives, have demonstrated exceptional NLO responses. Hybrid materials, combining organic and inorganic components, have also been explored to leverage the advantages of both material types. Recent breakthroughs in nanotechnology have enabled the precise tuning of material properties at the nanoscale, leading to the development of highly efficient NLO materials with tailored properties for specific applications. Additionally, the incorporation of dopants and the formation of composite materials have further enhanced the performance of NLO materials, making them more versatile and effective for a wider range of technological applications.

Xiaojun Li et al. found that Li_3NM molecules favorably interact with the triangular holes on the π -conjugated graphdiyne (GDY) surface, with van der Waals forces enhancing structural stability. The $\text{Li}_3\text{NLi@GDY}$ complex shows the highest binding energy, indicating strong interactions. NBO analysis reveals an increase in NPA charges from Li to K, leading to electron transfer and the formation of D- π -A pairs. The first hyperpolarizabilities increase with the atomic radius of alkali metals, with $\text{Li}_3\text{NK@GDY}$ showing exceptionally high values ($\sim 2.88 \times$

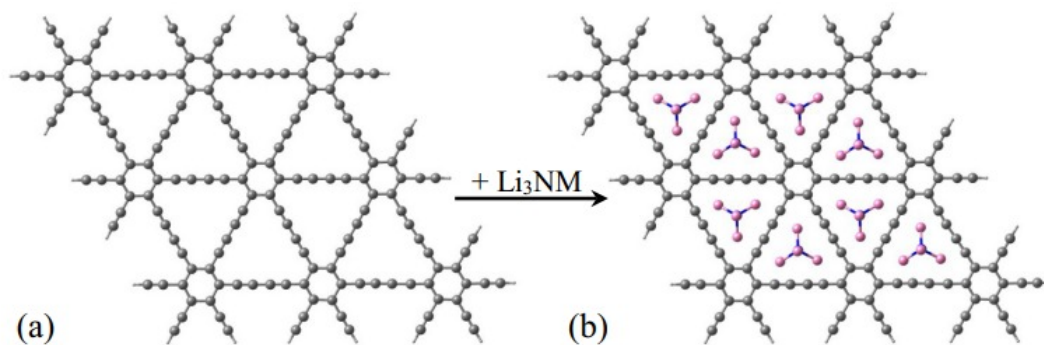


Figure 2.1: Schematic diagram of a functionalized graphdiyne (GDY) sheet adsorbed by the tetrahedral Li_3NM ($M = \text{Li}, \text{Na}, \text{K}$) alkalide complex

10^5 a.u.), suggesting these functionalized GDY structures are promising candidates for advanced NLO materials[34].Figure 2.1

K. Shehzadi et al.[35] built a new set of superalkali-doped graphdiyne (GDY) complexes with electron donor-acceptor frameworks, called $\text{M}_2\text{X}@\text{GDY}$ (where $M = \text{Li}, \text{Na}, \text{K}$ and $X = \text{F}, \text{Cl}, \text{Br}$). These were created using density functional theory (DFT) calculations. The findings demonstrate the stability of these complexes, as well as their greatly improved polarizability and initial hyperpolarizability up to 7.7×10^4 a.u. and decreased HOMO-LUMO gaps as shown in Table 2.1. These complexes are transparent to ultraviolet light, according to time-dependent DFT (TD-DFT) calculations, which offers information for the synthesis of new GDY-based nonlinear optical materials.

Density functional theory (DFT) was employed to calculate the optimized geometrical parameters, atomic charges, vibrational wavenumbers, and intensities of vibrational bands. Vibrational frequencies were scaled and compared with experimental FT-IR and FT-Raman spectra, showing excellent agreement with calculations based on B3LYP/6-311++G(d,p). The study also included electronic properties using TD-DFT, analyzing HOMO and LUMO energies, frontier molecular orbitals (FMO), molecular electrostatic potential (MEP), and thermodynamic properties. Mulliken charges, natural bond orbitals (NBOs), and NMR chemical shifts were calculated and compared with experimental data. Additionally, dipole moment, linear polarizability, and first hyperpolarizability values were computed.[23]

Density functional theory (DFT) calculations reveal that Li-doped boron nitride nanocones (BN-NCs) exhibit significantly enhanced second-order nonlinear optical (NLO) properties compared to non-doped BNNCs.[18] The electron density is effectively localized around the Li and neigh-

Table 2.1: Polarizability (α_0) in au, first hyperpolarizability (β_0) in au, change in dipole moment ($\Delta\mu$) in Debye, oscillator strength (f_0) in au, transition energy (ΔE) in eV, and second order hyperpolarizability (β_{vec}) of superalkali-doped graphdiyne ($M_2X@GDY$) complexes.

Complexes	(ω B97XD)		(LC-BLYP)		$\Delta\mu$	f_0	ΔE	β_{vec}
	α_0	β_0	α_0	β_0				
Pure GDY	441	2.13	413	0.74	0.0	0.87	4.23	0.55
Li ₂ F@GDY	585	1.91×10^4	561	1.30×10^4	0.16	0.34	2.83	1.12×10^4
Na ₂ F@GDY	604	6.6×10^4	584	7.7×10^4	0.33	0.60	3.10	6.9×10^4
K ₂ F@GDY	594	5.36×10^4	563	5.45×10^4	0.05	0.61	3.11	4.2×10^4
Li ₂ Cl@GDY	560	9.47×10^3	532	6.36×10^3	0.14	0.33	2.89	6.17×10^3
Na ₂ Cl@GDY	608	2.97×10^4	579	2.7×10^4	0.29	0.55	2.85	1.49×10^4
K ₂ Cl@GDY	594	3.33×10^4	655	3.04×10^4	0.15	0.24	2.76	2.09×10^4
Li ₂ Br@GDY	547	6.23×10^3	519	4.38×10^3	0.11	0.27	2.94	4.05×10^3
Na ₂ Br@GDY	600	5.00×10^4	577	5.6×10^4	0.27	0.60	3.16	4.78×10^4
K ₂ Br@GDY	600	4.47×10^4	568	4.49×10^4	0.35	0.58	3.14	3.91×10^4

boring B atoms, resulting in large static first hyperpolarizabilities. Time-dependent DFT results indicate pronounced charge transfer from BNNC to Li atoms, while the frequency-dependent effect on hyperpolarizabilities is minimal, making these materials promising candidates for advanced NLO applications as shown in the Figure 2.2.

Using density functional theory (DFT) computations, novel superalkali-based alkalides Li₃O@[12-crown-4]M were designed as excess electron compounds. QTAIM studies indicate non-covalent interactions between the complexant and alkali/superalkali clusters. These thermodynamically stable complexes exhibit significant interaction energies (33.40–44.23 kcal mol⁻¹) and narrow HOMO-LUMO gaps (0.17–0.27 eV) as shown in Figure 2.3. They display remarkable hyperpolarizability responses, with β_{4o} values ranging from 9.30×10^6 to 5.26×10^8 au, influenced by alkali metal size. The dynamic NLO response, particularly for the EOPE effects, shows a notable increase at 532 nm. The second hyperpolarizability response for the dc-Kerr constant reaches up to 2.75×10^{12} au, surpassing previously reported alkalides[40].

F. Ullah et al. performed DFT calculations, novel Group III phosphide (XY)₁₂ ($X = Al, B; Y = P$) nanoclusters are theoretically designed and investigated through exohedral doping with alkaline earth metals (Be, Mg, Ca). Doping significantly narrows the HOMO-LUMO gaps by

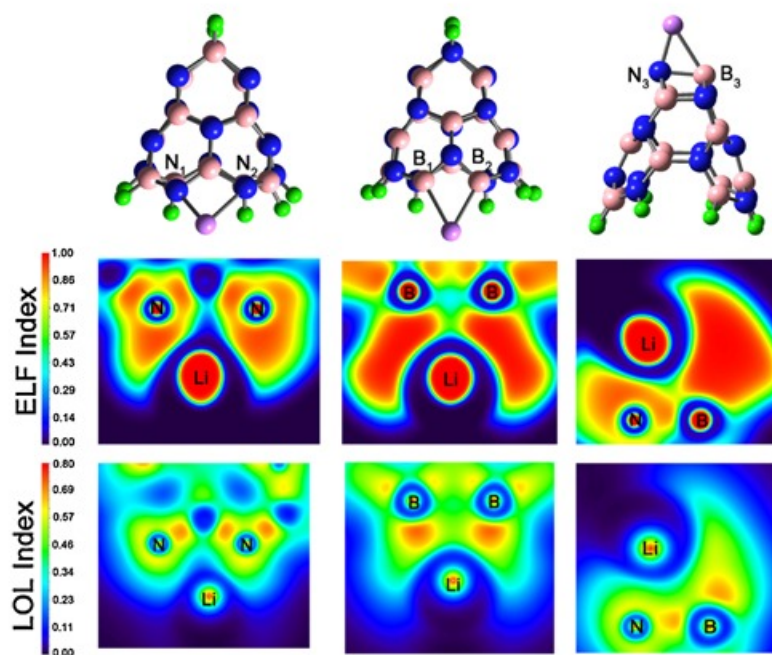


Figure 2.2: ELF and LOL analysis of Li@2N-BNNC, Li@2B-BNNC, and Li@BN-BNNC

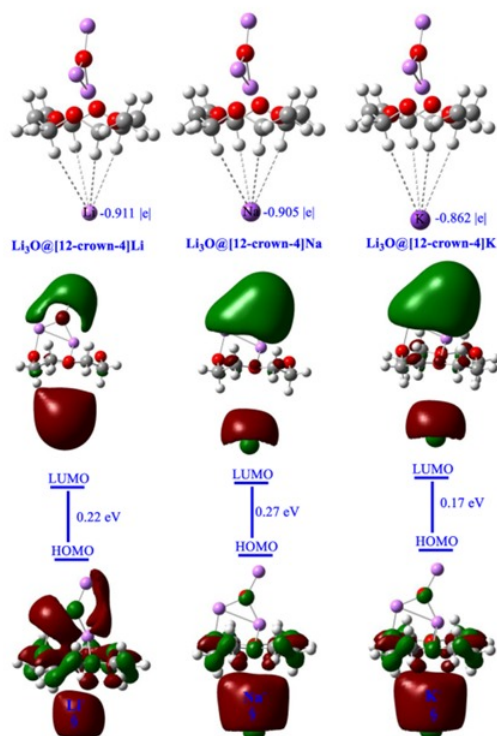


Figure 2.3: Optimized geometries with HOMO-LUMO densities of $\text{Li}_3\text{O@[12-crown-4]M}$ complexes.

raising the HOMO energy levels and shifts excess electrons from the metal atoms to the nanocluster, disrupting its centrosymmetry. This doping markedly enhances the nonlinear optical (NLO) response, with first hyperpolarizabilities (β_0) reaching up to 7.8×10^4 au, compared to the zero β_0 value of the undoped nanocage 2.4. These findings suggest potential applications in novel opto-electronic and high-performance NLO materials, warranting further experimental research.[36]

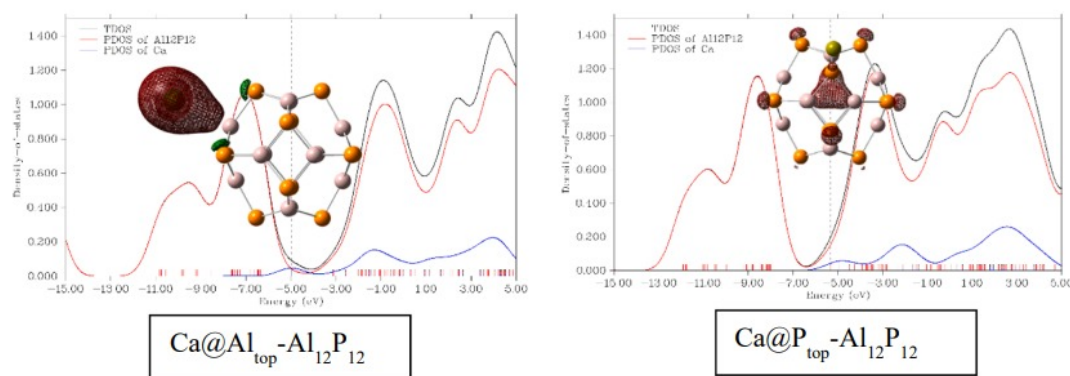


Figure 2.4: PDOS for Al/BP nanocages doped with various alkaline earth metals

A new strategy is utilized for enhancing nonlinear optical (NLO) response by utilizing a unique molecular salt structure. It focuses on how the σ chain $(\text{CH}_2)_4$ bridge, $\text{NH}_2 \cdots \text{M}/\text{M}_3\text{O}$ ($\text{M} = \text{Li}$, Na , and K) donors, and the electron hole cage $\text{C}_{20}\text{F}_{19}$ acceptor interact to promote long-range excess electron transport. The work shows how to successfully create electroneutral molecular salts with extra electron-hole pairs, exhibiting a notable NLO reaction.[15]

To achieve substantial NLO responses, the push-pull mechanism of excess electron production and its long-range transfer from the donor to the acceptor over the bridge are emphasized as crucial elements. Interestingly, the $\text{e}^- @ \text{C}_{20}\text{F}_{19} - (\text{CH}_2)_4 - \text{NH}_2 \cdots \text{Na}^+$ structure shows a significant initial hyperpolarizability (β_0) of up to 9.5×10^6 au, suggesting that the suggested A-B-D method works.[16]

Pandey et al. discussed recent advancements in the theoretical design and characterization of various superalkali-based compounds and their potential applications. They highlighted novel superalkalis for CO_2/N_2 capture and storage and analyzed the first-order hyperpolarizability-based nonlinear optical (NLO) responses of fullerene-like superalkali-doped $\text{B}_{12}\text{N}_{12}$ and $\text{B}_{12}\text{P}_{12}$ nanoclusters, which exhibit good ultraviolet (UV) transparency. Additionally, they examined a superalkali-based CaN_3Ca system, noting its high sensitivity as an alkali-earth-based aromatic multi-state NLO molecular switch. The review also covered the interactions of superalkalis

in both gas and liquid phases. The authors hope their review will inspire new experimental synthesis and practical applications of superalkalis and related compounds.[42]

Recently, Bano et al. conducted theoretical studies demonstrating that mixed superalkali clusters exhibit lower vertical ionization energies (2.81–3.36 eV) than alkali metals and Li₃O, making them excellent sources of excess electrons. Theoretical studies on mixed superalkali cluster-doped B₁₂N₁₂ nanocages show high interaction energies, smaller HOMO–LUMO energy gaps, and significant charge transfer. These complexes, stable and transparent in the UV region, have notable near-infrared absorption maxima. Complex C's first hyperpolarizability is vastly higher than pure Li₃O-doped B₁₂N₁₂, with impressive second hyperpolarizability values reflecting enhanced NLO responses. Additionally, the quadratic nonlinear refractive index values indicate these nanoclusters' potential for high-performance NLO materials[41].

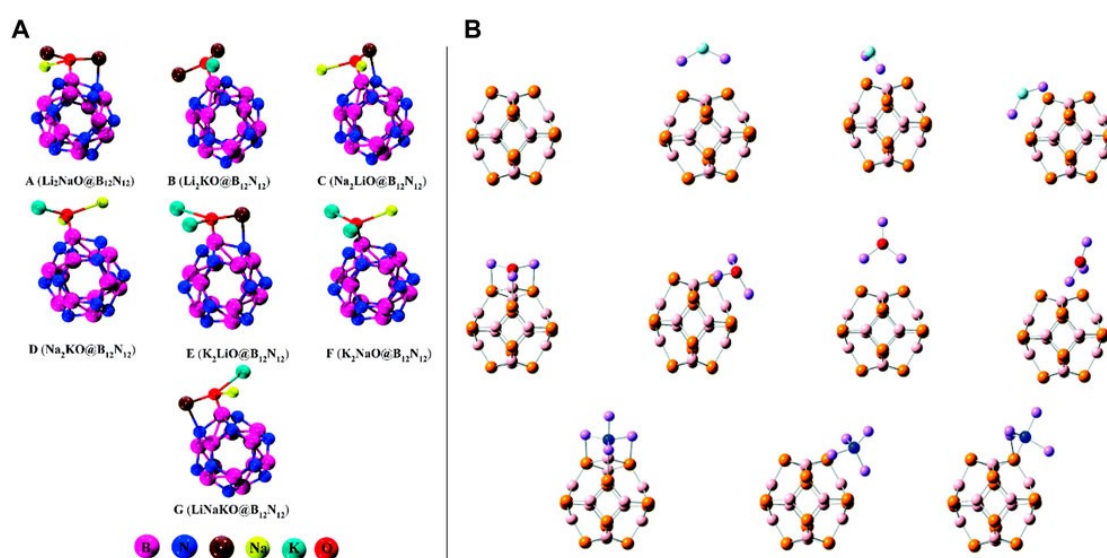


Figure 2.5: Optimized structures of the most stable mixed-superalkali-doped B₁₂N₁₂ complexes, as adapted from Bano et al. (2022), with permission from the Royal Society of Chemistry

Graphdiyne quantum dots (GDQDs) have notable electronic, optical, and electrochemical properties but suffer from low conductivity and quantum yield. Here, nitrogen-doped GDQDs (N-GDQDs) synthesized via a one-step hydrothermal method exhibit enhanced quantum yield (from 14.6% to 48.6%) and conductivity. These N-GDQDs are employed to construct an optical-electrochemical nanosensor for detecting dopamine (DA), achieving a detection limit of 0.14 M in fluorescence quenching and 0.02 M in electrochemical detection. The method demonstrates high accuracy in DA detection in human serum samples, indicating significant practical potential.[16]

Recent theoretical studies have focused on phosphide nano-cages with compositions MXP and MXP (where X represents either boron or aluminum, and M denotes alkali metals such as lithium, sodium, or potassium) to explore their geometric, electronic, and nonlinear optical (NLO) properties. The introduction of alkali metals, either by substituting aluminum or boron atoms or phosphorus atoms, has been shown to significantly alter the electronic and NLO characteristics of these nano-cages.[25]

One of the notable changes observed is a reduction in the HOMO-LUMO gap, accompanied by a substantial increase in the first hyperpolarizability of the doped AIP and BP nano-cages. This enhancement in NLO properties is attributed to the diffuse excess electrons contributed by the alkali metal dopants, as revealed by Partial Density of States (PDOS) analysis. Furthermore, Time-Dependent Density Functional Theory (TD-DFT) calculations have been utilized to investigate the impact of alkali metal doping on the optical absorption spectra, showing a red shift in the UV-visible region across all the studied nano-cages.[20]

Comparative analysis with nitride nano-cages indicates that alkali metal doping results in a greater enhancement of hyperpolarizability and NLO response in nitride nano-cages than in phosphide nano-cages. These findings underscore the potential of alkali metal-doped nano-cages in advancing the design of materials with tailored electronic and NLO properties for various applications [22].

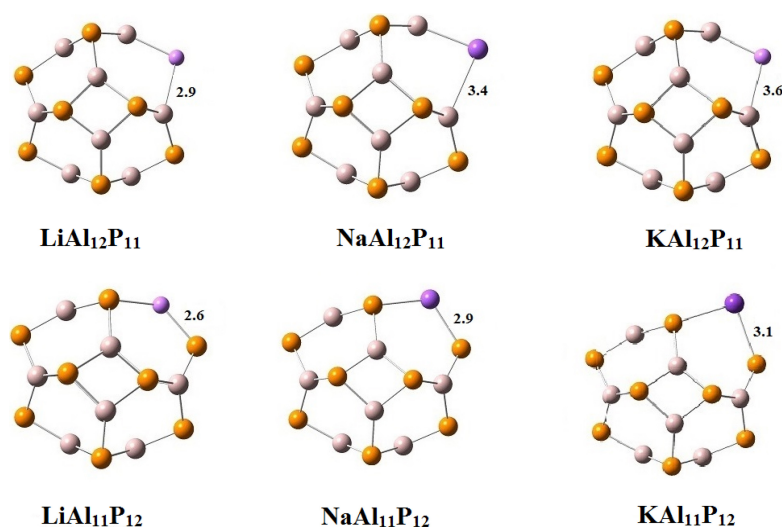


Figure 2.6: Optimized structures of alkali-doped AIP nano-cages ($\text{MA}_{12}\text{P}_{11}$ and $\text{MA}_{11}\text{P}_{12}$), with all bond lengths expressed in Angstroms.

Density Functional Theory (DFT) calculations reveal that Li atom complexation with $\text{B}_{12}\text{N}_{12}$

and $B_{16}N_{16}$ nanoclusters significantly narrows their HOMO-LUMO gaps and enhances their first hyperpolarizabilities, with increases up to 130,837 a.u. These findings suggest that Li-complexed BN nanoclusters have potential as advanced electro-optical materials [1].

Bimetallic superalkali clusters exhibit exceptional first hyperpolarizabilities (β_0), positioning them as promising candidates for next-generation nonlinear optical materials. Thermodynamically stable with binding energies ranging from 1.12 to 47.84 kcal mol⁻¹, these clusters show reduced HOMO-LUMO gaps and transparency in the deep UV region. Their hyperpolarizability values reach up to 4.3×10^4 a.u., with static second hyperpolarizability values as high as 6.1×10^7 a.u., indicating their potential for advanced NLO applications [4]. Push-pull functionalized fullerenes, featuring multiple N,N-diethylamine donors attached to N-methylpyrrolidine derivatives of C_{60} , were designed and analyzed. Density Functional Theory (DFT) calculations revealed that these fullerene derivatives exhibit increased polarizabilities, dipole moments, and first hyperpolarizabilities with additional N,N-Dimethylanilin groups. Time-Dependent DFT (TD-DFT) studies show a bathochromic shift in absorption spectra due to decreased transition energies. These complexes, with significant charge transfer characteristics, are promising as second-order nonlinear optical chromophores [3]. This study investigates the nonlinear optical properties of Au@Ag bimetallic nanoparticles synthesized via a seed-mediated method. Gold seeds with an 18 nm diameter were first prepared using a citrate-assisted thermal reduction process, followed by silver ion reduction with ascorbic acid. The nanoparticles were characterized using UV-Vis spectrophotometry, SEM, and Z-scan techniques with a 514 nm Argon CW laser. Results show that Au@Ag core-shell nanoparticles exhibit both negative and positive nonlinear absorption coefficients, and a negative nonlinear refraction index. Additionally, the nonlinear optical properties can be finely tuned by adjusting the shell thickness [30].

The study explores the electrical and optical properties of boron nitride nanocages doped with superalkali (OLi_3) and superhalogen (MgF_3). Both physical and substitutional doping methods are employed to assess the geometric and optoelectronic effects. The results show a significant increase in linear optical polarizability and nonlinear optical hyperpolarizability in the doped nanocages. The hyperpolarizability enhancement correlates with the atomic characteristics of the superhalogen and superalkali metals. Additionally, doping introduces new energy levels near the Fermi level, leading to a decrease in the HOMO-LUMO energy gap. Among the tested combinations, MgF_3 and OLi_3 doped with $B_{12}N_{10}$ demonstrate the most pronounced improvements in optical properties. These findings suggest potential applications of boron nitride nanocages in advanced electrical and nonlinear optical materials [24].

Molecules or clusters with diffuse excess electrons often exhibit significant nonlinear optical (NLO) properties, presenting new opportunities in material science. Over the past two decades, considerable effort has gone into designing and characterizing these compounds. This chapter summarizes recent computational studies on such molecules and clusters, offering insights into design strategies. It aims to assist in the future theoretical design and experimental synthesis of novel NLO materials utilizing the concept of excess electrons [28].

Using DFT and TD-DFT methods at the WB97XD/6-31G(d,p) level, this study investigates the potential of $B_{12}N_{12}$ nanocages for adsorbing and detecting cyanogen fluoride (FCN) in the presence of $1H^+$, $2H^+$, and $3H^+$ ions, as well as a static electric field (SEF). Structural and electronic parameters, adsorption energy, quantum descriptors, QTAIM, RDG, nonlinear optical (NLO) properties, UV–Visible transitions, and thermodynamic parameters were computed. The results show that the adsorption is exothermic with negative adsorption energy (E_{ads}), enthalpy (H), and Gibbs free energy (G). The bandgap energy of the FCN/ $B_{12}N_{12}$ complex decreases with increased H^+ ion functionalization and SEF, enhancing conductivity and sensitivity. The QTAIM, ELF, LOL, and RDG analyses confirm strong covalent bonding between FCN and $B_{12}N_{12}$. Notably, the $3H^+$ -functionalized $B_{12}N_{12}$ with FCN displays optical activity, and the application of a 700×10^{-3} a.u. SEF proves effective for detecting FCN as a toxic gas **ref8+**. Exploring materials with exceptionally large nonlinear optical (NLO) responses is a compelling scientific challenge. This study investigates alkali metal-doped $Zn_{12}O_{12}$ nanocages, identified as inorganic electrides with remarkable NLO properties. Density Functional Theory (DFT) calculations were used to analyze the geometric, electronic, and NLO responses of both exo- and endohedrally doped $Zn_{12}O_{12}$ nanoclusters. For exohedral doping, various alkali metal positions were considered, revealing that the electride nature of the complexes depends on the doping site. All exohedral complexes, except for doping on six-membered rings (r_6), exhibit electride characteristics. Interaction energies indicate that all doped nanoclusters are thermodynamically stable, except for endo-K@ $Zn_{12}O_{12}$. The exothermic nature of alkali metal encapsulation contrasts with the endothermic encapsulation observed in other inorganic fullerenes. The study also evaluates barriers for interconversion between exo- and endohedral complexes. Alkali metal doping significantly reduces the HOMO-LUMO gap and enhances hyperpolarizability by several orders of magnitude. Notably, exohedrally doped complexes show higher NLO responses than endohedral ones, with the highest first hyperpolarizability of 1.0×10^5 a.u. observed for K@ r_6 - $Zn_{12}O_{12}$. The third-order NLO responses were compared with leading systems reported in the literature [31].

2.2 Problem Statement

Graphdiyne exhibits promising non linear optical properties but its performance is currently limited by factors such as centrosymmetry and structural stability under high intensity light in order to achieve maximum polarizability and hyperpolarizability value .

2.3 Solution statement

A possible strategy to root out the above concern is by designing novel 2D graphdiyne by doping and functionalization of GDY material with different adsorbates or hybridization with other nanomaterials to enhance its polarizability and hyperpolarizability value. These novel complexes will provide promising candidate for designing novel GDY-based NLO materials.

2.4 Research Goals and Aims

1. To investigate Germanium doped graphdiyne complex through DFT calculations.
2. To monitor change of NLO properties of GDY as a result of doping and adsorption of superalkalis.
3. To rationalize polarizability and Hyperpolarizability trend in Ge-doped GDY.

CHAPTER 3

Methodology

3.1 Computational Simulation Suite

Molecular modeling, often known as computational chemistry, is a set of methods for using a computer to explore chemical problems. It employs theoretical methods within sophisticated computer programs to analyze and predict the structures and properties of molecules

flow chart

Computational chemistry methods can be divided into

- i. Classical Mechanical Method
- ii. Quantum Mechanical Method

3.2 Classical Mechanical Method

Classical mechanical methods use two approaches to address the properties of molecules on a large scale.

A) Molecular Mechanics B) Molecular Dynamics

3.2.1 Molecular Mechanics

Molecular mechanics relies on classical physics to predict the structure and properties of molecules. It is employed to analyze static properties, such as structural characteristics and the energy of minimum energy structures. MM methods are fast, computationally inexpensive, and less com-

plex, making them suitable for handling very large systems, such as enzymes. These methods evaluate the potential energy surface for the regular arrangement of atoms, allowing for the prediction of molecular energy, equilibrium geometry, transition states, and relative energies of various conformers."

3.2.2 Molecular Dynamics

Molecular dynamics is a computer simulation technique that models the physical movement of atoms and molecules. It utilizes force fields to generate dynamic properties, such as the evolution of structure over time, by calculating the forces and velocities of atoms

3.3 Quantum Mechanical Method

Quantum mechanical methods are grounded in the Schrödinger wave equation and operate on the principle of wave-particle duality of electrons. These methods employ two main approaches to address properties at the smallest scale

- 1) Wave Functional based Theory
- 2) Density Functional Theory

3.3.1 Wave Functional based Theory

Wave function theory relies entirely on the wave function, a mathematical function encompassing all the characteristics of the system. This theory employs three fundamental approaches to address its principles[6].

- i) Hartee-Fock Method
- ii) Semi-empirical Method
- iii) Electron-Correlated Method

3.3.2 Density Functional Theory

Density functional theory (DFT) is a computational quantum mechanical modeling method used to explore various electronic properties of ground state systems[38]. These properties include geometry optimization, spectroscopic analysis (IR, UV, and NMR), single-point energy calcu-

lations, potential energy surfaces, dipole moments, atomic charges, mechanistic studies, and time-dependent calculations. Unlike wave function theory, which focuses entirely on the wave function, DFT treats the energy of a molecule as a functional of electron density, which depends on the x, y, and z coordinates.

Density functional theory (DFT) is a widely used method to solve the many-body Schrödinger equation, based on the Hohenberg-Kohn and Kohn-Sham theorems. In DFT, a functional dependent on the electron density is employed to characterize the properties of many-electron systems

3.3.3 The Hohenberg-Kohn theorem

The central theorem of DFT is based on the Hohenberg-Kohn theorems. based on the two fundamental theorems that follow Fro any many-body system of interacting electrons exposed to an external potential $V_{ext}(r)$, the ground state particle density $n_0(r)$ uniquely sets the external potential $V_{ext}(r)$. It indicates that there is a unique functional $n_0(r)$ associated with the ground state electron density [6].

According to quantum mechanics, the complete information about the electronic structure and properties of a molecule can be obtained from the wave function using the Schrödinger Wave equation for systems with multiple nuclei and electrons

$$\hat{H}\Psi = E\Psi \quad (3.3.1)$$

Ψ = many-electron wave function

E = Eigenvalue of the operator (total energy of the system)

\hat{H} = Hamiltonian operator

3.3.4 Kohn- Sham Equations

The Kohn-Sham (KS) ansatz simplifies the complex problem of interacting N-particles into a more manageable single-particle, non-interacting problem. According to the Kohn-Sham the-

ory, the ground state density of a system can be described by non-interacting particles moving under the influence of an effective potential.[21]

$$V_r = V_{\text{ext}}(r) + \frac{1}{2} \sum_{i \neq j} \quad (3.3.2)$$

Where $V_{\text{ext}}(r)$ is the external potential acting on the interacting system, the electron-electron Coulomb interaction is represented by the second term, and the exchange-correlation potential, which encapsulates all many-body exchange and correlation effects, is presented in the third term. The exchange-correlation functional $E_{\text{xc}}[n(r)]$ is the only component that needs to be evaluated. The difference between the many-body problem and the single-particle problem is characterized by $n(r)$. The Kohn-Sham orbitals depend on the effective potential, which in turn depends on the electron density, creating a dependency loop. Therefore, to find the ground state, the electron density-dependent Kohn-Sham equation must be solved in a self-consistent manner.

3.4 ADF Simulation Suite

ADF Modelling suite has been used to study the adsorption of superalkali clusters on Germanium doped GDY. Quantum mechanical simulations based on DFT approach were performed using ADF modelling suit with GGA/PBE functional and tripple zeta basis set. [7] GGA/PBE is one of most popular functional in DFT studies for surface adsorption phenomenon. Initially, geometry optimization of pristine GDY containing 30 carbon atoms and 12 hydrogen atom is performed to get the most stable structure with lowest possible ground state energy. DFT calculations are performed running simulations using ADF modelling suit, after completion of successful simulations, adsorption energies, HOMO-LUMO gap values, electrical conductivity and charges are calculated. Furthermore, other parameters including chemical potential, chemical hardness, electron affinity, ionization energy are determined to analyze the efficient adsorption.

3.5 Computational Tool

The Amsterdam Density Functional (ADF) is a computational chemistry program that utilizes advanced molecular Density Functional Theory (DFT) to address chemical problems[7]. It predicts structures, reactivity, and molecular spectra, enabling accurate modeling of properties for nanoparticles, organic materials, and transition metal complexes. ADF can precisely handle

all elements of the periodic table using the ZORA relativistic approach and Slater Type Orbital (STO) all-electron basis sets.

3.5.1 Functionality

- Single Point Calculation
- Geometry Optimization
- Transition States
- Frequencies and Thermodynamic Properties
- Tracing a Reaction Path
- Computation of any Electronic Configuration
- Excitation Energies, Oscillator Strengths, Transition Dipole Moments, (Hyper)Polarizabilities, Van der Waals Dispersion Coefficients, CD Spectra, ORD, using Time-Dependent Density Functional Theory (TDDFT)
- ESR (EPR) g-Tensors, A-Tensors, NQCCs
- NMR Chemical Shifts and Spin-Spin Coupling Constants
- Various other Molecular Properties
- Treatment of Large Systems and Environment by the QM/MM (Quantum Mechanics / Molecular Mechanics) Hybrid Approach

3.5.2 The Hohenberg-Kohn theorem

The central theorem of DFT is based on the Hohenberg-Kohn theorems based on the two fundamental theorems that follow

Theorem I:

For any many-body system of interacting electrons exposed to an external potential $V_{\text{ext}}(\mathbf{r})$, the ground state particle density $n_0(\mathbf{r})$ uniquely sets the external potential $V_{\text{ext}}(\mathbf{r})$. It indicates that there is a unique functional $n_0(\mathbf{r})$ associated with the ground state electron density n .

Theorem II:

A global total energy function, defined with the external potential $V_{\text{ext}}(r)$ and particle density $n(r)$, can be used to determine $E[n]$ for any specific $V_{\text{ext}}(r)$. The ground state energy of the system corresponds to the global minimum value of this functional, and the density that minimizes it is precisely the system's ground state density, denoted by $n_0(r)$ [21].

The total energy function is expressed as follows:

$$E[n(r)] = F_{\text{HK}}[n(r)] + \int V_{\text{ext}}(r)n(r) dr \quad (3.5.1)$$

The functional $F_{\text{HK}}[n(r)]$ encompasses the electronic kinetic energy and all electron-electron interaction terms. Theorem I underscores the significance of the ground-state density in determining all ground-state properties of a system. According to Theorem II, $F_{\text{HK}}[n(r)]$, which applies to all N -electron systems, is a universal functional. The external potential $V_{\text{ext}}(r)$ is unique to each specific system, and thus, the Hamiltonian is fully determined by $V_{\text{ext}}(r)$, which is, in turn, completely defined by the ground-state particle density $n_0(r)$.

3.5.3 Exchange Coorelation Functionals

To formulate and solve the exchange-correlation functional, a few approximations are necessary. The exchange-correlation functional, $E_{xc}[n(r)]$, consists of electron correlations and electron exchange. Here, we present two of the most commonly used approximations for the exchange-correlation functional.

3.5.4 The Local Density Approximation

The Local Density Approximation (LDA) is an approach to the exchange-correlation energy functional in DFT. In this approximation, the functional depends solely on the local electron density at a specific point, assuming the electron density is uniformly distributed throughout the molecule.[21]

3.5.5 Generalized Gradient approximations

In Generalized Gradient Approximation (GGA), the functional considers both the electron density and its gradient. This method accounts for the non-uniform distribution of electrons throughout the system, calculating the exchange-correlation functional based on the electron density at

each point r and its gradient.[21]

3.6 Methodology

ADF can calculate various solid-state properties, some of which are discussed below

- The band structure of complex materials can be studied using DFT to determine indirect and direct band gaps for detailed analysis.
- Electron density plots can reveal charge transfer between different atoms in a material
- Magnetic properties, including spin-up and spin-down density of states and magnetic moment values, can be calculated.
- The density of states (DOS) of a material can be analyzed to observe the total DOS and the partial DOS contributions from specific orbitals, such as s, p, d, and f, depending on the k-mesh.

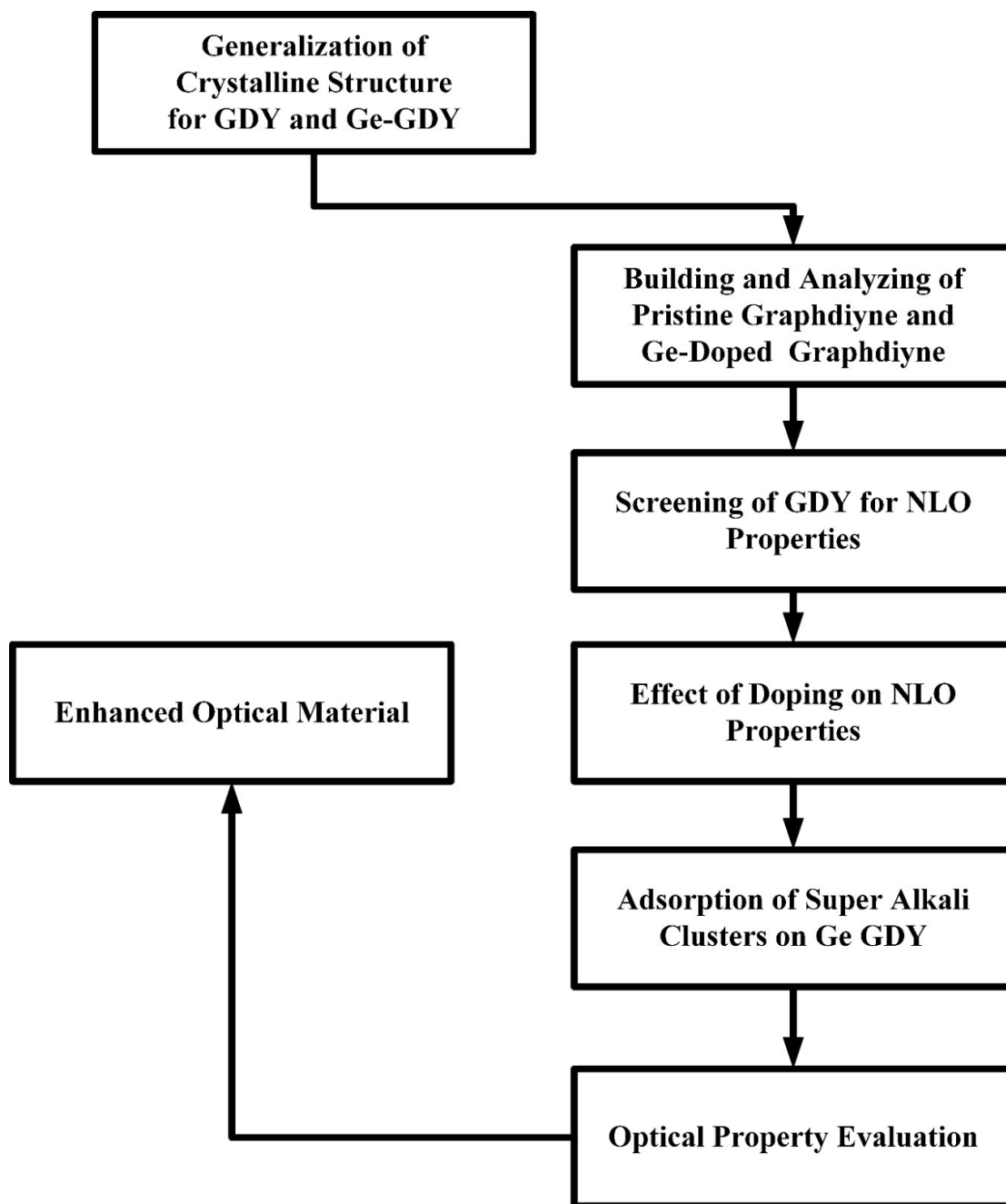


Figure 3.1: Step-based methodology for current research

Results And Discussion

4.1 Quantum Mechanical Investigation of graphdiyne

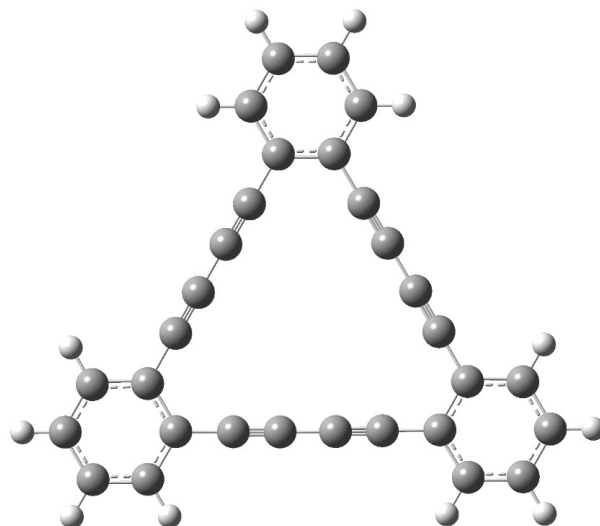
This Chapter discusses the results obtained for adsorption of superalkali cluster on doped graphdiyne using computational approaches to investigate the structural stability, electronic, magnetic and NLO properties. The study of Ge doped GDY was performed by using periodic DFT. The simulations were carried out using a 3D unit cell of GDY that contained 30 carbon atoms and 12 hydrogen atoms. Calculations were made for the adsorption energies, electronic parameters, and density of states of AM_3O on Ge doped GDY. Pristine GDY, Ge doped GDY and AM_3O ($AM=Li,Na,K$) were optimised using GGA-PBE functional with TZ (Triple zeta) basis set using ADF modelling suit to examine the adsorption at discrete atomic level.

For our study, we employed the following equations to compute the adsorption energy[33]

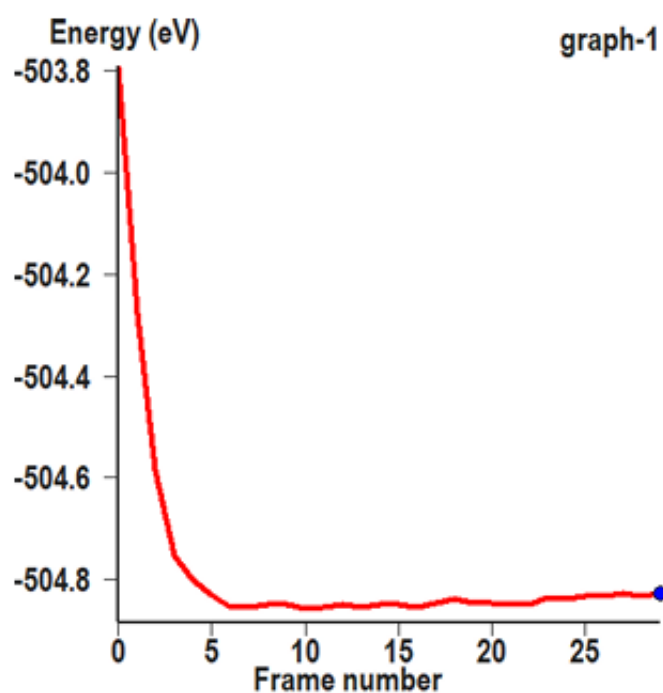
$$\Delta E_{\text{ads}} = E_{\text{Ge-GDY}/AM_3O} - (E_{\text{Ge-GDY}} + E_{AM_3}) \quad (4.1.1)$$

4.2 Geometry Optimization

Geometry optimization and electrical characteristics were obtained using Density Functional Theory (DFT). Theoretical simulations were conducted on Germanium doped GDY using the ADF modeling suite. DFT calculations were performed with a tripple zeta (TZ) basis set and the GGA: PBE method at 298 K. The optimized structures and their corresponding graphs are presented below in Figure 4.1 - 4.5



[a]

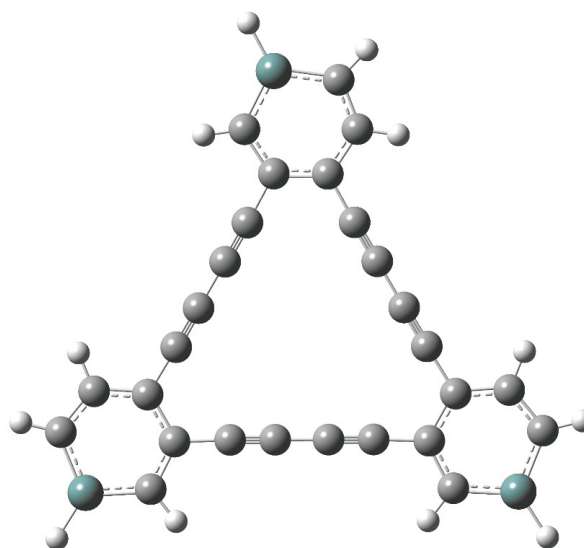


[b]

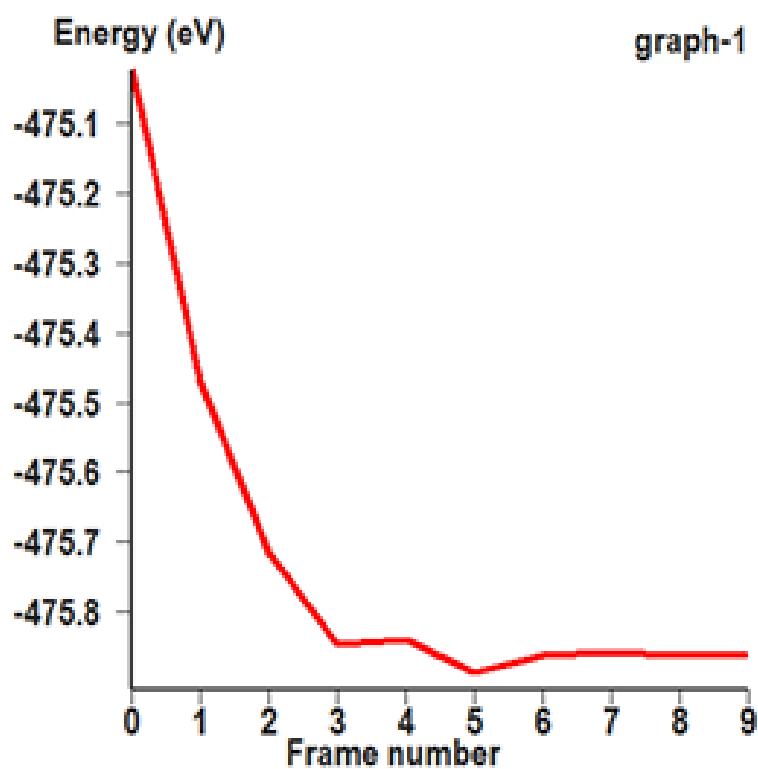
Figure 4.1: [a]Optimized geometry of pristine GDY, [b]Energy graph of pristine GDY calculated at TZ basis set at GGA: PBE/DFT performed at ADF modelling suite

4.3 Adsorption Energy

To elaborate, the interaction energies (E_{int}) of superalkalis with graphdiyne and the stabilities of the resulting complexes are calculated. The highest interaction energy of 3.06 eV (Table 4.1) is



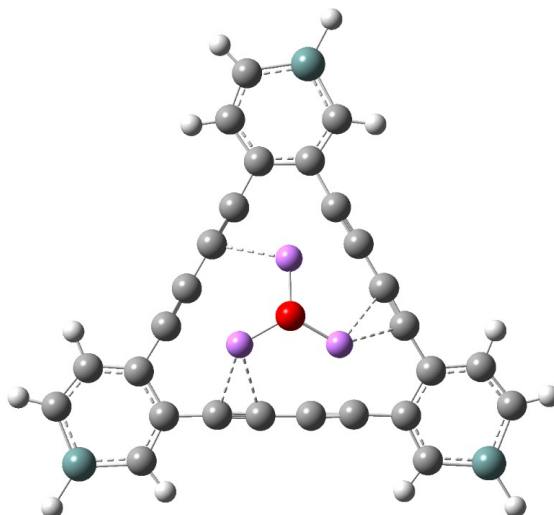
[a]



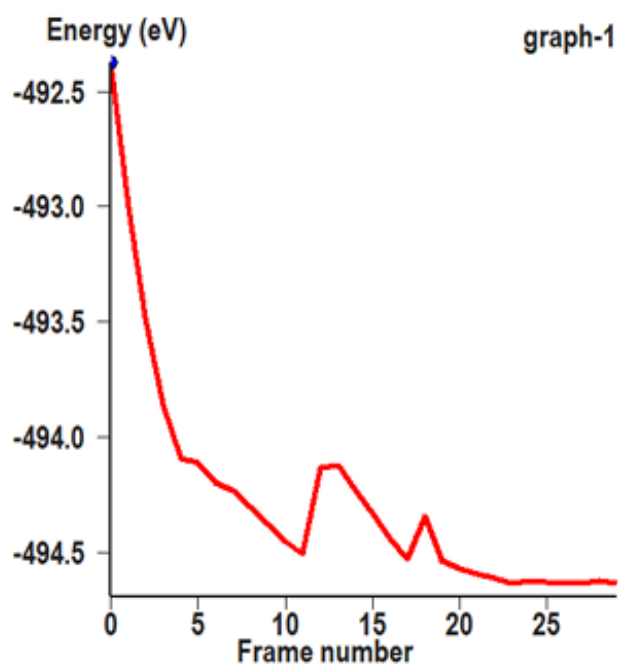
[b]

Figure 4.2: [a] Optimized geometry of Ge doped GDY, [b]Energy graph of Ge doped GDY calculated at TZ basis set at GGA: PBE/DFT performed at ADF modelling suite

observed for $\text{Li}_3\text{O}@$ Ge-GDY which indicates the high stability as well as strong interaction of Li_3O (superalkali) with graphdiyne. The interaction energy values of 2.84 eV and 2.79 eV are



[a]



[b]

Figure 4.3: [a] Optimized geometry of Li_3O on Ge doped GDY and [b]energy graph of Li_3O on Ge doped GDY calculated at TZ basis set at GGA: PBE/DFT performed at ADF modelling suite

calculated for Na_3O and K_3O , respectively. Concluded that interaction energy decreases with increase in atomic size of superalkalis because of weak van der waals forces.

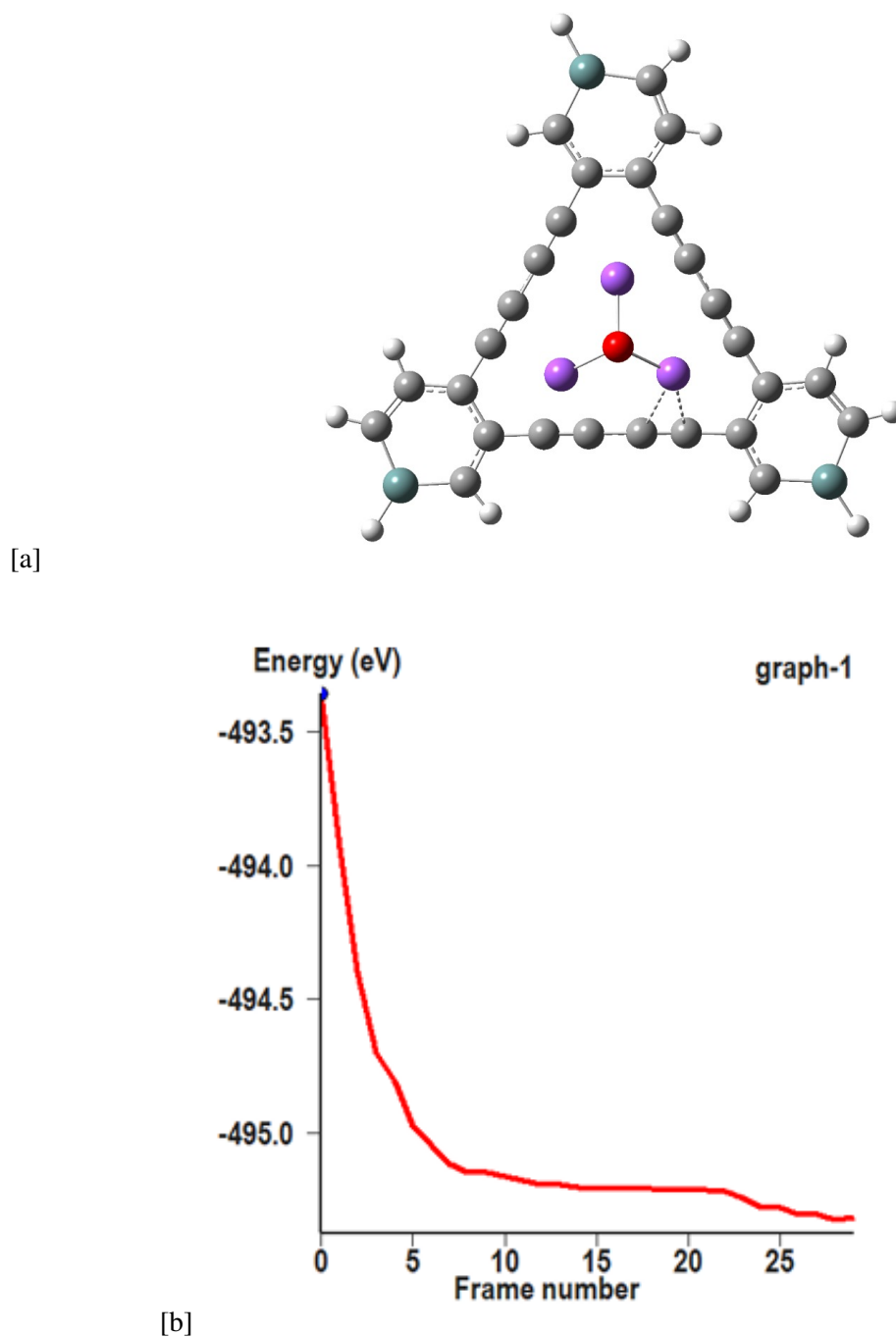
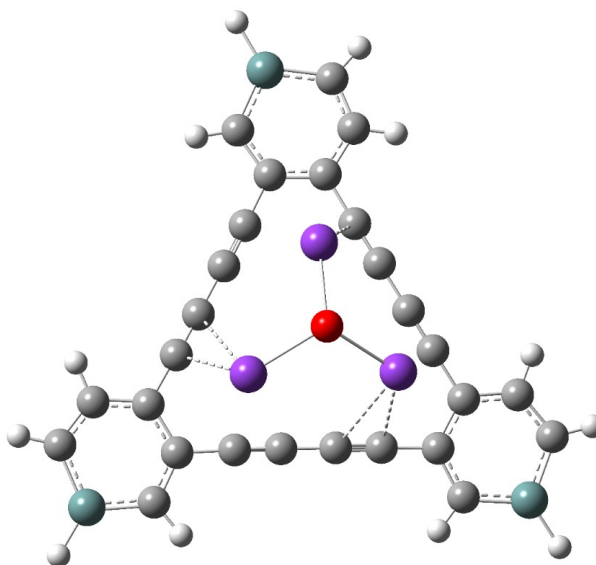


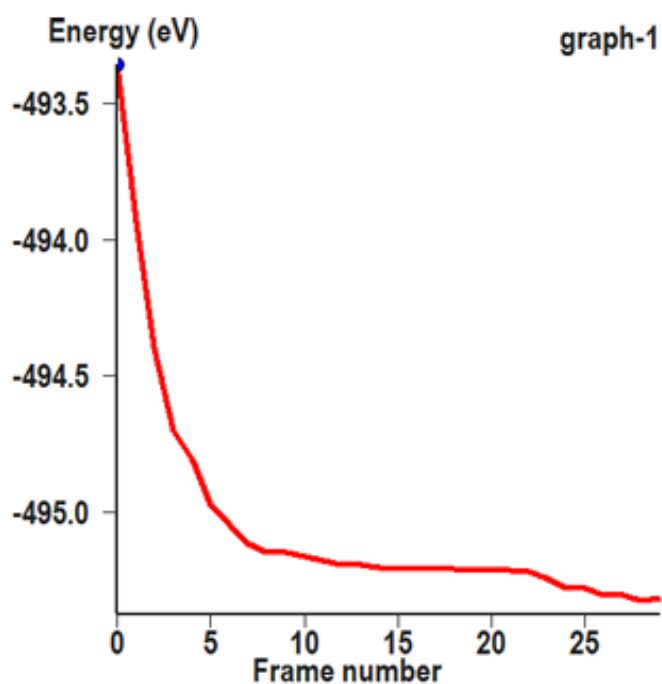
Figure 4.4: [a] Optimized geometry of Na_3O on Ge doped GDY and [b]energy graph of Na_3O on Ge doped GDY calculated at TZ basis set at GGA: PBE/DFT performed at ADF modelling suite

4.3.1 Adsorption behavior at elevated temperature i-e 323 K

Through DFT calculations, structure stability and performance at a higher temperature of 323 K was analyzed. Different superalkali metals (AM_3O) are adsorbed on Ge-doped GDY surfaces



[a]



[b]

Figure 4.5: [a] Optimized geometry of K_3O on Ge doped GDY and [b] energy graph of K_3O on Ge doped GDY calculated at TZ basis set at GGA: PBE/DFT performed at ADF modelling suite

while maintaining this elevated temperature i-e 313K. The results indicate that increased temperature does not compromise structure stability but rather enhances the NLO response of Ge doped GDY structures. Table 4.2

Table 4.1: The adsorption energy values of GDY clusters at 298 K

Clusters	$E_{Complex}$ (eV)	E_{Ge-GDY} (eV)	E_{AM3} (eV)	$E_{adsorption}$ (eV)
Li ₃ O / Ge doped GDY	-205.61	-182.77	-19.78	-3.06
Na ₃ O / Ge doped GDY	-201.44	-182.77	-15.83	-2.84
K ₃ O / Ge doped GDY	-198.37	-182.77	-12.81	-2.79

Table 4.2: The adsorption energy values of superalkali clusters at 313 K

Clusters	$E_{Complex}$ (eV)	E_{GDY} (eV)	E_{AM3} (eV)	$E_{adsorption}$ (eV)
Li ₃ O/Ge doped GDY	-205.65	-182.77	-19.78	-3.10
Na ₃ O/Ge doped GDY	-201.47	-182.77	-15.83	-2.87
K ₃ O/Ge doped GDY	-198.39	-182.77	-12.81	-2.81

4.4 Frontier molecular orbital(FMO) analysis

Conductivity, resistivity, and electronic properties are assessed through frontier molecular orbital (FMO) analysis. The highest occupied molecular orbital (HOMO) and the lowest unoccupied molecular orbital (LUMO) are essential in quantum chemistry for predicting molecular interactions. HOMO, being electron-rich, often donates electrons, while LUMO, with its empty spaces, can accept electrons. The HOMO's energy inversely relates to the ionization potential, and LUMO's energy inversely correlates with the electron affinity.[12] The energy gap (E_g) between HOMO and LUMO indicates the structure's stability and reactivity. The energy value of HOMO-LUMO orbitals and energy difference are reported in Table 4.3 and orbital isosurface in Figures 4.6 and 4.8

The H-L gap results show that the pure graphdiyne (GDY) is an insulator material with large H-L gap value (4.15eV). However, the value is reduced with doping of Germanium (3.123 eV). Doping Graphdiyne with Germanium atoms introduces new energy levels within the band gap of the pristine graphdiyne making the material more conductive and enhancing its electronic properties. Furthermore, these values are reduced with superalkali doping on Ge-GDY surface. Li₃O @Ge-GDY shows H-L gap value of 0.506eV while Na₃O @Ge-GDY and K₃O @Ge-GDY shows 0.437eV and 0.231eV respectively. This reduction in the HOMO-LUMO gap indicates the formation of new HOMO orbitals between the original HOMO and LUMO orbitals, with the valence electrons of the superalkalis playing a key role in this process. Essentially, superalkalis decrease the HOMO-LUMO gap by transferring their valence electrons to

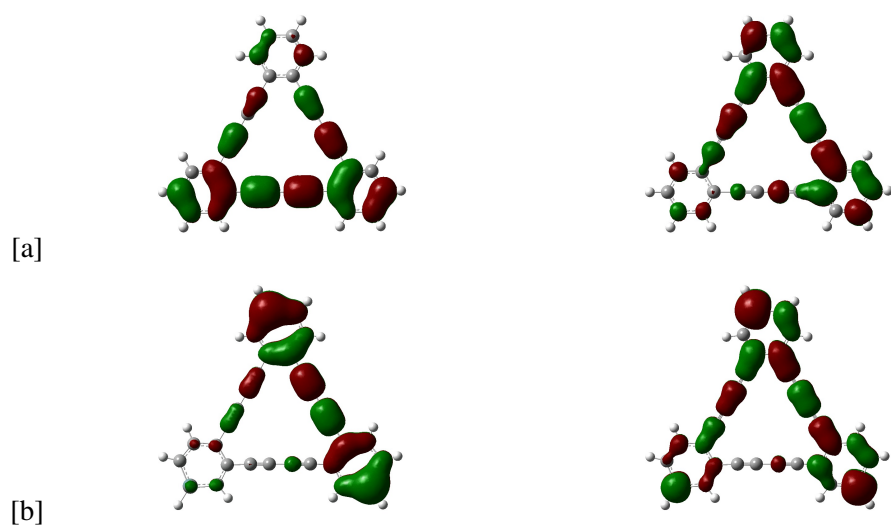


Figure 4.6: HOMO-LUMO representation of (a)pristine GDY (b)Ge-GDY

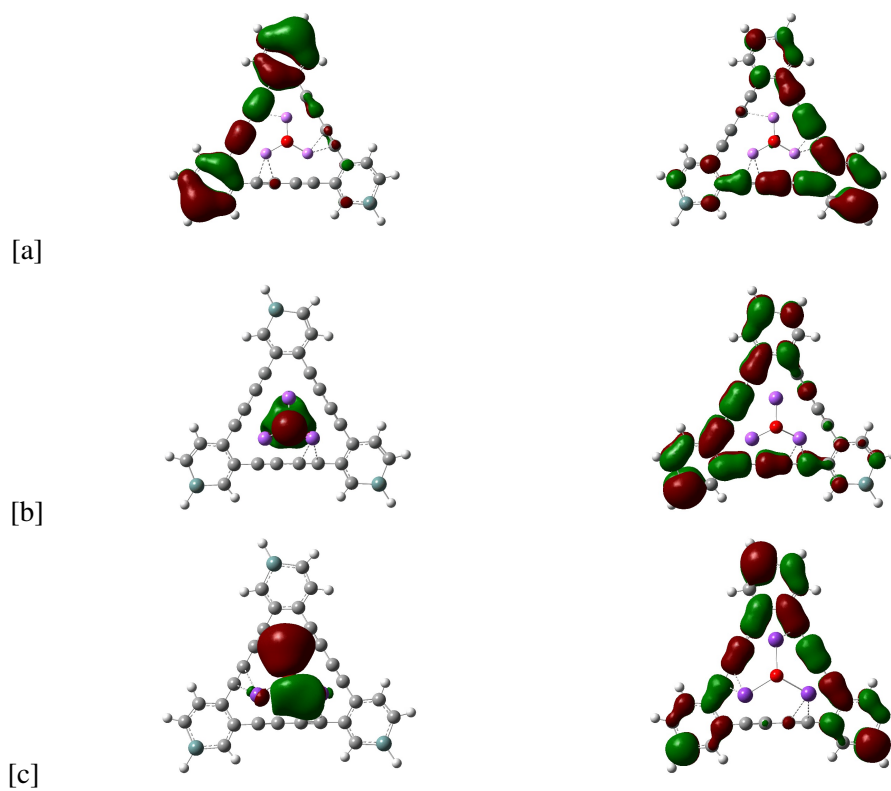


Figure 4.7: HOMO-LUMO representation of (a) $\text{Li}_3\text{O}/\text{Ge-GDY}$ (b) $\text{Na}_3\text{O}/\text{Ge-GDY}$ (c) $\text{K}_3\text{O}/\text{Ge-GDY}$

GDY.

Table 4.3: HOMO-LUMO energy values of pristine and Ge doped GDY clusters of superalkalis

Cluster	E_{HOMO} (eV)	E_{LUMO} (eV)	$\delta E_{LUMO-HOMO}$ (eV)
GDY	-7.852	-3.701	4.15
Ge-GDY	-6.304	-3.181	3.123
Li ₃ O/ Ge-GDY	-1.466	-0.960	0.506
Na ₃ O / Ge-GDY	-1.251	-0.814	0.437
K ₃ O/Ge-GDY	-0.073	0.158	0.231

4.5 Charge Transfer mechanism

4.5.1 Natural Bond Orbital(NBO) analysis

NBO analysis was performed to study the charge transfer in the superalkali-doped complexes. The NBO charge values for these complexes range from 0.27 to 0.32 e^- , significantly higher than the charge of pure GDY (0.0 e^-). Our calculated results depict that charge transfer takes place from the superalkali cluster to GDY, resulting in the superalkali acquiring a positive charge. This also confirms the intermolecular electron donor-acceptor (D- π -A) process. Additionally, an overall increase in the charge of the superalkali is observed with an increase in atomic number, attributed to the decrease in ionization potential down the group.

The electronic stabilities of the complexes can also be confirmed by calculating their vertical ionization energies (VIE). The VIE results, as shown in Table 4.5, indicate that when the AM₃O clusters are adsorbed on the delocalized GDY surface, the VIE values of the adsorbed GDY clusters gradually decrease from Li to K in the range of 3.983–4.303 eV. The K₃O@Ge-GDY cluster has a relatively smaller VIE value (3.983 eV), which is also lower than the ionization potential (4.34eV) of the K atom. The designed alkalides possess significant VIE values, which indicate their electronic stability. Consequently, these adsorbed GDY complexes with lower VIEs can be considered novel superalkali complexes and may produce a significant nonlinear optical response.

4.5.2 Natural Population Analysis

The natural analysis method offers an alternative to the traditional Mulliken population analysis. It appears to provide enhanced numerical stability and a more accurate depiction of electron distribution, particularly in compounds with high ionic character, such as those containing metal atoms[6]. The natural charges attained by O atoms of adsorbate are largely negative from -0.274 to -0.774|e| while the charges on alkali metal atoms are 0.119–0.526|e|. Therefore, the total positive charges (Q_{tot} , ranging from 0.087 to 0.980|e| on the AM_3O indicate strong alkali-like characteristics for the complexes studied. Furthermore, these results indicate that the AM_3O unit behaves similarly to an alkali metal atom and donates an electron to the GDY cluster. It is also observed that the Na atom holds a larger positive charge in the adsorbed GDY clusters compared to the other two alkali metals, following the order: $Q_K > Q_{Na} > Q_{Li}$. However, the total charges (Q_{tot}) on the AM_3O unit increase gradually from Li to K, which aligns with the decreasing vertical ionization.

Table 4.4: Charge values for different clusters adsorbed on GDY.

Clusters	Q_{AM1}	Q_{AM2}	Q_{AM3}	Q_O	Q_{tot}
$Li_3O@GDY$	0.122	0.120	0.119	-0.274	0.587
$Na_3O@GDY$	0.526	0.524	0.525	-0.774	0.680
$K_3O@GDY$	0.363	0.368	0.365	-0.432	0.964

4.6 Nonlinear optical properties

The presence of excess electrons in any system can significantly enhance the nonlinear optical response. These excess electrons reduce the HOMO-LUMO gap by occupying the high-energy HOMO orbitals of the corresponding system, leading to an increase in first hyperpolarizability values. The NLO properties of $AM_3O@Ge$ -GDY complexes have been explored by calculating mean polarizabilities (α_0) and static hyperpolarizabilities (β_0) as shown in Table 4.5. Our calculated value of polarizability for pure GDY is 440 au, and this value is enhanced when germanium is doped on the GDY surface. In $AM_3O@Ge$ -GDY complexes, α_0 for $Li_3O@Ge$ -GDY is 585 au, which further increases to 604 au for $Na_3O@Ge$ -GDY and 640 au for $K_3O@Ge$ -GDY. It is evident that α_0 of $AM_3O@Ge$ -GDY increases as the atomic number of AM increases. Therefore, the mean polarizability of previously studied AM_3O complexes is smaller than those of

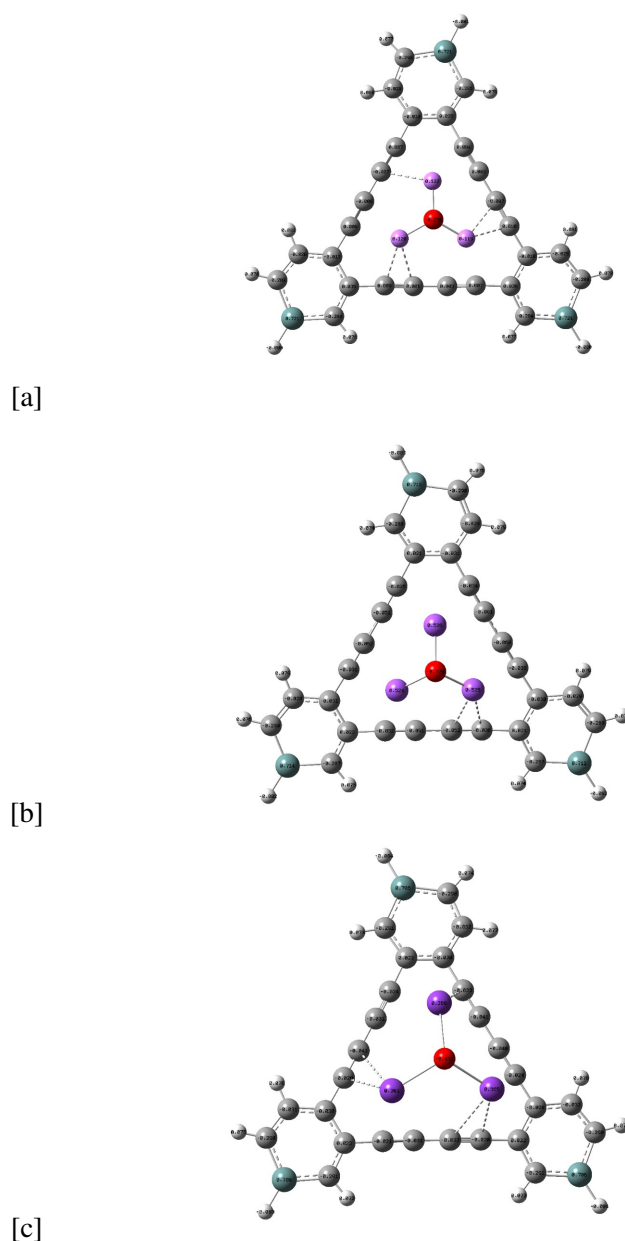


Figure 4.8: Charge Analysis of (a) $\text{Li}_3\text{O}/\text{Ge-GDY}$ (b) $\text{Na}_3\text{O}/\text{Ge-GDY}$ (c) $\text{K}_3\text{O}/\text{Ge-GDY}$

$\text{AM}_3\text{O}@/\text{Ge-GDY}$ complexes reported here.

The increase in static polarizability of any system is sensitive to the delocalization of valence electrons. This means that the presence of more dispersed electrons in the HOMO orbitals leads to an increase in the α_0 values. The increase in α_0 values shows an interesting trend in the β_0 values of $\text{AM}_3\text{O}@/\text{Ge-GDY}$ complexes. For instance, $\text{Li}_3\text{O}@/\text{Ge-GDY}$ has a β_0 of 1.91×10^4 au, which further increases for $\text{Na}_3\text{O}@/\text{Ge-GDY}$ and reaches its highest for $\text{K}_3\text{O}@/\text{Ge-GDY}$. Static polarizability of any system is expressed as

$$\beta_{\text{tot}} \propto \frac{\Delta\mu f_0}{\Delta E^3} \quad (4.6.1)$$

where $\Delta\mu$ and ΔE^3 are transition dipole moments and energies for crucial excited states, which is the state with the largest oscillator strengths (f_0) [22]

The mean dipole moment (μ_o), static polarizability (α_o), the static first hyperpolarizability (β_{tot}) and average second hyperpolarizability (ave) are expressed as follows

$$\mu_0 = (\mu_x^2 + \mu_y^2 + \mu_z^2)^{1/2} \quad (4.6.2)$$

$$\alpha_0 = \frac{\alpha_{xx} + \alpha_{yy} + \alpha_{zz}}{3} \quad (4.6.3)$$

$$\beta_{\text{tot}} = (\beta_x^2 + \beta_y^2 + \beta_z^2)^{1/2} \quad (4.6.4)$$

Table 4.5: Calculated vertical ionization potentials (VIP), the HOMO-LUMO gaps (E_g), mean dipole moment (μ_o) in a.u., static polarizability (α_o) in a.u., the static first hyperpolarizability (β)_{tot} in a.u.

Clusters	VIP	E_g (eV)	μ_o	α_o	β_{tot}
Pristine GDY	7.056	4.15	0.00	492.04	0.86
Ge doped GDY	7.013	3.123	1.43	534.26	73.4
Li ₃ O@Ge-GDY	4.303	0.506	1.58	798.72	28304.28
Na ₃ O@Ge-GDY	4.100	0.437	1.73	812.91	336543.37
K ₃ O@Ge-GDY	3.983	0.231	1.67	845.34	5393051

4.7 Electrical Conductivity

Electrical conductivity is a measure of a material's ability to conduct electric current. It quantifies how easily electrons can flow through a material when an electric field is applied. Conductivity is typically denoted by the symbol (σ) and is the reciprocal of electrical resistivity, which measures how strongly a material opposes the flow of electric current. The value of energy gap (E_g) between HOMO and LUMO determines the material's conductivity.

The relationship between conductivity and E_g value is shown as

$$\sigma = e^{-\Delta E/2kT}$$

where

$$\Delta E = E_{HOMO} - E_{LUMO}$$

In this expression:

- σ is the electrical conductivity.
- ΔE is the energy gap (often denoted as E_g).
- k is the Boltzmann constant.
- T is the absolute temperature.

Energy gap and electrical conductivity are determined for AM_3O adsorption on the surface of Pristine GDY and Ge doped GDY. Computing results indicate that GDY with Ge doping exhibits a smaller energy gap and higher electrical conductivity Table 4.6. The reduced energy gap facilitates the rapid transition of electrons from the valence band to the conduction band, enabling electrical conductivity.

array

Table 4.6: Electronic parameters and electrical conductivity of Ge-GDYs

Cluster	E_{HOMO} (eV)	E_{LUMO} (eV)	$\delta E_{LUMO-HOMO}$ (eV)	Electrical Conductivity S/m $\sigma = e^{-\frac{\Delta E}{2kT}}$
GDY	-7.852	-3.701	4.15	3.66×10^{-34}
Ge-GDY	-6.304	-3.181	3.123	6.870×10^{-26}
Li ₃ O/ Ge-GDY	-1.466	-0.960	0.506	8.374×10^{-5}
Na ₃ O / Ge-GDY	-1.251	-0.814	0.437	0.00030142
K ₃ O/Ge-GDY	-0.073	0.158	0.231	0.01376

4.8 Global Quantum Chemical Descriptors

We calculated the global indices for our systems to evaluate the energy stabilization when they gain an additional electronic charge from the environment. Based on the HOMO and LUMO energy values, ionization potential (I), electron affinity (A), softness (S), hardness (η), chemical potential (μ), softness (S), electronegativity (χ), and electrophilicity index (ω) are determined.

$$\text{Ionization Potential (I)} = -E_{\text{HOMO}} \quad (4.8.1)$$

$$\text{Electron Affinity (A)} = -E_{\text{LUMO}} \quad (4.8.2)$$

$$\text{Chemical Hardness } (\eta) = \frac{I - A}{2} \quad (4.8.3)$$

$$\text{Chemical Potential } (\mu) = -\frac{I + A}{2} \quad (4.8.4)$$

$$\text{Softness (S)} = \frac{1}{2\eta} \quad (4.8.5)$$

$$\text{Electronegativity } (\chi) = \frac{I + A}{2} \quad (4.8.6)$$

$$\text{Electrophilicity } (\omega) = \frac{\mu^2}{2\eta} \quad (4.8.7)$$

Table 4.7: Global indices for the complexes

Complex	I (eV)	A (eV)	η (eV)	μ (eV)	χ (eV)	S (eV)	ω (eV)
Pristine GDY	7.852	3.701	2.075	-5.776	5.776	0.240	8.039
Ge doped GDY	6.304	3.181	1.561	-4.742	4.742	0.320	7.202
Li ₃ O/ Ge-GDY	1.466	0.960	0.253	-1.213	1.213	1.976	2.907
Na ₃ O/ Ge-GDY	1.251	0.814	0.218	-1.032	1.032	2.293	2.442
K ₃ O/ Ge-GDY	0.073	-0.158	0.115	0.042	-0.042	4.347	0.007

CHAPTER 5

Conclusion

The functionalized graphdiyne (GDY) structures doped with Germanium atoms and adsorbed by AM_3O units (where $AM = Li, Na, K$) have been investigated using DFT calculations for exploring the NLO properties as potential optical materials. The AM_3O units exhibit strong interactions with the Ge-GDY clusters, as indicated by the large binding energies observed for Li adsorbed complex i.e. -3.06eV while the K_3O -adsorbed Ge-GDY structure is stabilized by van der Waals interactions. The HOMO-LUMO gap values calculated were 0.506eV , 0.437eV , and 0.231eV for $Li_3O@Ge-GDY$, $Na_3O@Ge-GDY$, $K_3O@Ge-GDY$ respectively. Moreover, the adsorption of superalkalis on Ge doped GDY significantly reduce the H-L gap in all complexes. The results reveal that the adsorption of AM_3O onto Ge-GDY significantly lowers the vertical ionization potential (VIP) of the species, and intramolecular charge transfer plays a crucial role in determining the nonlinear optical (NLO) properties. Interestingly, Doped complexes show an outstanding NLO response with significantly high first hyperpolarizability values ranging from 2.83×10^4 au to 5.39×10^6 au when compared with pure graphdiyne. In conclusion, the adsorption of AM_3O onto Ge-GDY enables the optimization of the NLO response of GDY-based materials, facilitating the design of advanced optoelectronic materials with high NLO properties for future applications.

Future Perspective

The enhancement of nonlinear optical (NLO) responses in germanium-doped graphdiyne modulated by superalkali clusters holds significant promise for the future of photonics, quantum computing, and optoelectronics. This material could lead to more efficient NLO devices such as optical switches and modulators, which are vital for telecommunications and optical computing. Additionally, its potential in quantum information processing and optoelectronic devices like photodetectors and LEDs offers prospects for next-generation technologies. Further experimentation with different doping elements beyond germanium, or varying the concentration of dopants, could lead to optimized NLO properties. Exploring co-doping strategies, where multiple dopants are introduced simultaneously, might also offer a way to achieve even more pronounced NLO responses. Beyond superalkali clusters, other types of clusters (e.g., superhalogens, metal-organic frameworks) could be investigated for modulating NLO properties. This exploration could reveal new mechanisms for enhancing the optical responses of graphdiyne and similar materials. Tailoring material properties through doping and functionalization could allow for customized applications, while further research into synthesis and computational modeling could optimize its practical use. With applications ranging from environmental monitoring to nanophotonics and wearable technologies, germanium-doped graphdiyne presents opportunities for interdisciplinary research and innovation across various high-tech industries.

Bibliography

- [1] T. H. Maiman *et al.*, “Stimulated optical radiation in ruby,” 1960.
- [2] Y.-R. Shen, “Principles of nonlinear optics,” 1984.
- [3] P. F. Bordui and M. M. Fejer, “Inorganic crystals for nonlinear optical frequency conversion,” *Annual Review of Materials Science*, vol. 23, no. 1, pp. 321–379, 1993.
- [4] T. Kaino and S. Tomaru, “Organic materials for nonlinear optics,” *Advanced Materials*, vol. 5, no. 3, pp. 172–178, 1993.
- [5] J. Zyss and I. Ledoux, “Nonlinear optics in multipolar media: Theory and experiments,” *Chemical reviews*, vol. 94, no. 1, pp. 77–105, 1994.
- [6] W. Kohn and L. Sham, “Density functional theory,” in *Conference Proceedings-Italian Physical Society*, Editrice Compositori, vol. 49, 1996, pp. 561–572.
- [7] G. t. Te Velde, F. M. Bickelhaupt, E. J. Baerends, *et al.*, “Chemistry with adf,” *Journal of Computational Chemistry*, vol. 22, no. 9, pp. 931–967, 2001.
- [8] J. G. Grote, J. S. Zetts, R. L. Nelson, *et al.*, “Nonlinear optic polymer electro-optic modulators for space applications,” in *Photonics for Space Environments VIII*, SPIE, vol. 4823, 2002, pp. 6–18.
- [9] T. Vijayakumar, I. H. Joe, C. R. Nair, and V. Jayakumar, “Efficient π electrons delocalization in prospective push–pull non-linear optical chromophore 4-[n, n-dimethylamino]-4-nitro stilbene (dans): A vibrational spectroscopic study,” *Chemical Physics*, vol. 343, no. 1, pp. 83–99, 2008.
- [10] E. G. Lewars, “Computational chemistry,” *Introduction to the theory and applications of molecular and quantum mechanics*, vol. 318, 2011.

BIBLIOGRAPHY

- [11] A. Orbelli Biroli, F. Tessore, M. Pizzotti, *et al.*, “A multitechnique physicochemical investigation of various factors controlling the photoaction spectra and of some aspects of the electron transfer for a series of push–pull zn (ii) porphyrins acting as dyes in dsscs,” *The Journal of Physical Chemistry C*, vol. 115, no. 46, pp. 23 170–23 182, 2011.
- [12] M. Govindarajan and M. Karabacak, “Spectroscopic properties, nlo, homo–lumo and nbo analysis of 2, 5-lutidine,” *Spectrochimica Acta Part A: Molecular and Biomolecular Spectroscopy*, vol. 96, pp. 421–435, 2012.
- [13] Y. Zhang, Q. Pei, and C. Wang, “Mechanical properties of graphynes under tension: A molecular dynamics study,” *Applied Physics Letters*, vol. 101, no. 8, 2012.
- [14] Q. Zheng, G. Luo, Q. Liu, *et al.*, “Structural and electronic properties of bilayer and trilayer graphdiyne,” *Nanoscale*, vol. 4, no. 13, pp. 3990–3996, 2012.
- [15] Y. Bai, Z.-J. Zhou, J.-J. Wang, *et al.*, “New acceptor–bridge–donor strategy for enhancing nlo response with long-range excess electron transfer from the nh2... m/m3o donor (m= li, na, k) to inside the electron hole cage c20f19 acceptor through the unusual σ chain bridge (ch2) 4,” *The Journal of Physical Chemistry A*, vol. 117, no. 13, pp. 2835–2843, 2013.
- [16] Y. Bai, Z.-J. Zhou, J.-J. Wang, *et al.*, “New acceptor–bridge–donor strategy for enhancing nlo response with long-range excess electron transfer from the nh2... m/m3o donor (m= li, na, k) to inside the electron hole cage c20f19 acceptor through the unusual σ chain bridge (ch2) 4,” *The Journal of Physical Chemistry A*, vol. 117, no. 13, pp. 2835–2843, 2013.
- [17] W.-M. Sun, L.-T. Fan, Y. Li, J.-Y. Liu, D. Wu, and Z.-R. Li, “On the potential application of superalkali clusters in designing novel alkalides with large nonlinear optical properties,” *Inorganic chemistry*, vol. 53, no. 12, pp. 6170–6178, 2014.
- [18] W.-Y. Wang, N.-N. Ma, C.-H. Wang, M.-Y. Zhang, S.-L. Sun, and Y.-Q. Qiu, “Enhancement of second-order nonlinear optical response in boron nitride nanocone: Li-doped effect,” *Journal of Molecular Graphics and Modelling*, vol. 48, pp. 28–35, 2014.
- [19] R.-L. Zhong, H.-L. Xu, Z.-R. Li, and Z.-M. Su, “Role of excess electrons in nonlinear optical response,” *The journal of physical chemistry letters*, vol. 6, no. 4, pp. 612–619, 2015.

BIBLIOGRAPHY

- [20] K. Ayub, "Are phosphide nano-cages better than nitride nano-cages? a kinetic, thermodynamic and non-linear optical properties study of alkali metal encapsulated x 12 y 12 nano-cages," *Journal of Materials Chemistry C*, vol. 4, no. 46, pp. 10919–10934, 2016.
- [21] J. G. Lee, *Computational materials science: an introduction*. CRC press, 2016.
- [22] E. Shakerzadeh, E. Tahmasebi, and Z. Biglari, "A quantum chemical study on the remarkable nonlinear optical and electronic characteristics of boron nitride nanoclusters by complexation via lithium atom," *Journal of Molecular Liquids*, vol. 221, pp. 443–451, 2016.
- [23] P. Vennila, M. Govindaraju, G. Venkatesh, and C. Kamal, "Molecular structure, vibrational spectral assignments (ft-ir and ft-raman), nmr, nbo, homo-lumo and nlo properties of o-methoxybenzaldehyde based on dft calculations," *Journal of Molecular Structure*, vol. 1111, pp. 151–156, 2016.
- [24] S. Altürk, D. Avcı, Ö. Tamer, and Y. Atalay, "Comparison of different hybrid dft methods on structural, spectroscopic, electronic and nlo parameters for a potential nlo material," *Computational and Theoretical Chemistry*, vol. 1100, pp. 34–45, 2017.
- [25] J. Iqbal, R. Ludwig, K. Ayub, *et al.*, "Phosphides or nitrides for better nlo properties? a detailed comparative study of alkali metal doped nano-cages," *Materials Research Bulletin*, vol. 92, pp. 113–122, 2017.
- [26] Z. Jia, Y. Li, Z. Zuo, H. Liu, C. Huang, and Y. Li, "Synthesis and properties of 2d carbon graphdiyne," *Accounts of chemical research*, vol. 50, no. 10, pp. 2470–2478, 2017.
- [27] X. Liu, Q. Guo, and J. Qiu, "Emerging low-dimensional materials for nonlinear optics and ultrafast photonics," *Advanced Materials*, vol. 29, no. 14, p. 1605886, 2017.
- [28] D. Hou, A. S. Nissimagoudar, Q. Bian, *et al.*, "Prediction and characterization of nagas2, a high thermal conductivity mid-infrared nonlinear optical material for high-power laser frequency conversion," *Inorganic Chemistry*, vol. 58, no. 1, pp. 93–98, 2018.
- [29] C. Huang, Y. Li, N. Wang, *et al.*, "Progress in research into 2d graphdiyne-based materials," *Chemical reviews*, vol. 118, no. 16, pp. 7744–7803, 2018.
- [30] X. Yang, X. Lin, Y. S. Zhao, and D. Yan, "Recent advances in micro-/nanostructured metal-organic frameworks towards photonic and electronic applications," *Chemistry—A European Journal*, vol. 24, no. 25, pp. 6484–6493, 2018.

BIBLIOGRAPHY

- [31] B. P. Biswal, S. Valligatla, M. Wang, *et al.*, “Nonlinear optical switching in regioregular porphyrin covalent organic frameworks,” *Angewandte Chemie International Edition*, vol. 58, no. 21, pp. 6896–6900, 2019.
- [32] F.-B. Chen, K.-L. Chi, W.-Y. Yen, J.-K. Sheu, M.-L. Lee, and J.-W. Shi, “Investigation on modulation speed of photon-recycling white light-emitting diodes with vertical-conduction structure,” *Journal of Lightwave Technology*, vol. 37, no. 4, pp. 1225–1230, 2019.
- [33] X. Gao, H. Liu, D. Wang, and J. Zhang, “Graphdiyne: Synthesis, properties, and applications,” *Chemical Society Reviews*, vol. 48, no. 3, pp. 908–936, 2019.
- [34] X. Li, “Graphdiyne: A promising nonlinear optical material modulated by tetrahedral alkali-metal nitrides,” *Journal of Molecular Liquids*, vol. 277, pp. 641–645, 2019.
- [35] K. Shehzadi, K. Ayub, and T. Mahmood, “Theoretical study on design of novel superalkalis doped graphdiyne: A new donor–acceptor ($d-\pi-a$) strategy for enhancing nlo response,” *Applied Surface Science*, vol. 492, pp. 255–263, 2019.
- [36] F. Ullah, N. Kosar, A. Ali, T. Mahmood, K. Ayub, *et al.*, “Alkaline earth metal decorated phosphide nanoclusters for potential applications as high performance nlo materials; a first principle study,” *Physica E: Low-dimensional Systems and Nanostructures*, vol. 118, p. 113 906, 2020.
- [37] R. Bano, M. Asghar, K. Ayub, *et al.*, “A theoretical perspective on strategies for modeling high performance nonlinear optical materials,” *Frontiers in Materials*, vol. 8, p. 783 239, 2021.
- [38] W. Hu and M. Chen, *Advances in density functional theory and beyond for computational chemistry*, 2021.
- [39] C. Trovatiello, A. Marini, X. Xu, *et al.*, “Optical parametric amplification by monolayer transition metal dichalcogenides,” *Nature Photonics*, vol. 15, no. 1, pp. 6–10, 2021.
- [40] A. Ahsin and K. Ayub, “Superalkali-based alkalides $Li_3O@[12\text{-crown-}4]_m$ (where $m = Li, Na, \text{ and } K$) with remarkable static and dynamic nlo properties; a dft study,” *Materials Science in Semiconductor Processing*, vol. 138, p. 106 254, 2022.
- [41] R. Bano, K. Ayub, T. Mahmood, *et al.*, “Mixed superalkalis are a better choice than pure superalkalis for $b_{12}n_{12}$ nanocages to design high-performance nonlinear optical materials,” *Dalton Transactions*, vol. 51, no. 21, pp. 8437–8453, 2022.

BIBLIOGRAPHY

- [42] S. K. Pandey, E. Arunan, R. Das, A. Roy, and A. K. Mishra, “Recent advances in in silico design and characterization of superalkali-based materials and their potential applications: A,” *Superhalogens & Superalkalis: Exploration of Structure, Properties and Applications*, 2022.